Synthetic Graphite and Graphene Nanoplatelets Composites for Electromagnetic Interference Shielding

A thesis submitted to the University of Manchester for the degree of

Master of Philosophy

In the Faculty of Science and Engineering

2022

Lina Jfairi

Department of Materials

Contents

Word count: 24,442

List of Figures

List of Tables

List of Abbreviations

EMC: Electromagnetic Compatibility

EMI: Electromagnetic Interference

EMIS: Electromagnetic Interference Shielding

EMISE: Electromagnetic Interference Shielding Effectiveness

EMS: Electromagnetic Shielding

EMW: Electromagnetic Waves

xGnP: Exfoliated Graphene Nanoplatelet

GIM: Graphite Intercalated Compounds

GNP: Graphene Nano-platelet

MagS: Magnetic Stirrer

MechS: Mechanical Stirrer

R1: Round 1

R2: Round 2

R3: Round 3

RAM: Radar Absorbing Material

SE: Shielding Efficiency

SG: Synthetic Graphite

Son: Sonicator

Abstract

This study looked to investigate the feasibility of using an insulative resin with a conductive filler to produce mediums that can attenuate or eliminate Electromagnetic Interference (EMI). The three conductive fillers examined were synthetic graphite (SG) and two classes of exfoliated graphene nanoplatelets (xGnP). A combination of xGnP composites composing of more than 10 layers of graphene and synthetic graphite (SG) nanocomposites were manufactured. The xGnP of more than 10-layer graphene composites, and the SG only composites were both subjected to two temperatures 34°C and 40°C, which were alternated throughout the repeated experimental processes, with stipulated steps in each experiment. The SG nanocomposites containing biodegradable compostable ingredients were manufactured using another composite manufacturing process that involved room temperature. Experiments using temperature treatments and associated steps were found to show normal tensile behaviour of epoxy composites using the Bluehill Universal software used in the Intron 3344 tensile testing machine. Compared to other epoxies having similar as Diglycidyl Ether Bisphenol A (DGBEA) and epichlorohydrin having the same molecular weight or repeats. The molecular weight of DGEBA and epichlorohydrin is ≈700g/mol. Conversely, the composites with food grade ingredients demonstrated greater ductility, and continued to stretch under the strain caused by the top grip compared to temperature treated experiments at 34°C and 40°C. All composites examined showed no conductivity, but on gentle polishing, several demonstrated a near zero resistance value i.e., very high conductance. A long lean cycle order was used for purposes of researching the alignment of the platelets using magnetic, standard exfoliation and sonication during cure.

DECLARATION

No portion of the work referred to in the thesis has been submitted in support of an

application for another degree or qualification of this or any other university or other

institute of learning.

http://www.library.manchester.ac.uk/about/regulations/) and in The University's

policy on Presentation of Theses.

Acknowledgement

It has been a journey of persistence, and due diligence. I have formerly studied my undergraduate degree (Textile Design and Design Management BSC achieving 2:1) at the University of Manchester. I appreciate all the hard work of all the staff who played a role in my learning.

Firstly, I would like to convey my special thanks to Dr Hugh Gong, for his sense of warm care and continued guidance. He is approachable, caring and devoted to his students.

Huge thanks to Mr. Stuart Morse for his help in The Mill Mechanical Testing Lab. He continued to be of good help when setting up the Instron instrumentation. Great thanks also go to Mr. Michael Faulkner for his kind explanation of the Scanning Electron Microscope (SEM) imagery technical observations. I also extend this special thanks to Dr Christopher Wilkins who kindly gave up his time to help train me with using the SEM.

Finally, my beloved mother who is endlessly dedicated to her family. She has instilled a strong sense of discipline in me. This trait is mirrored in my project supervisor and operatic vocal teacher. I am endlessly grateful to these three individuals that have been part of my journey thus far. Thank you for teaching me grit, a priceless teaching.

Chapter 1 – Introduction

1.1 Background

Conductive materials such as synthetic graphite and xGnP are needed in the vicinity of electromagnetic interference to stabilise and secure devices that vary in operation from modern life electronic devices to civil (inclusive of medical such as magnetic resonance imaging (MRI) equipment), historically in domestic devices where they are used as graphite brushes, in the military and aerospace equipment (Wang et al., 2021). Graphene and graphite fillers are used in electromagnetic shielding mediums as they are highly conductive reinforcements for composites in some polymer composites to protect sensitive electrical equipment in different industries as stated above.

Furthermore, through introducing graphene into composites, this therefore enhances the electrical, thermal, and electromagnetic properties of the composites, which would then likely improve the EMIS attenuation level of the composites.

However, the research gap of using graphene related filler is that in recent times researchers have seen that graphite and graphene-based materials that in order to obtain good electrical properties the percolation threshold is required to be or above 15%. As the percolation threshold is maximised, a loss of polymeric flexibility and some processing difficulties are exhibited, which means that some polymeric tensile properties of the composites are shown, this leads to brittle composites that will develop as with the increase of the filler percentage (Kumar et al., 2017).

Even though this type of research has been carried out, still there is this knowledge gap of using a variety of mixing mechanisms and processes, whether the variation of mixing methods would impact the alignment of the platelets within the composite, and whether heat would impact the tensile properties of the composites.

To find a solution to this research gap, the aim of my research is going to be research a variety of mixing methods both mechanically and with magnetised mixing, added to sonication to minimise the production of air pockets in the cured composites. The use of a variety of mixing methods would be to observe the behaviour of the platelets under the different conditions and how this would impact the properties of the final samples. This research aims to utilise both compostable and synthetic materials to determine whether the ratio of natural to synthetic ingredients, would add to the ductility of the epoxy resin. In-addition this thesis explores whether utilising a variety of composite manufacturing processes (chapter 3), and biodegradable ingredients for both the compostable combined nano composites, and the temperature conditioned composite experiments would have an impact on the mechanical properties of the composites. The different manufacturing processes used in this research are to study the behaviour of the fillers, combined with the thermoset insulative resin, whether these materials would have any behavioural impact on the conductivity of the specimens through the means of simple agitation, intercalation of xGnP, and SG platelets under room temperature or heat, and time conditions. However, the compostable combined nano composites enable the study of the influence of ratio in compostable ingredients over the integral nature of thermoset epoxy. This research cross-examines the effect of biodegradable food grade materials combined with epoxy and synthetic graphite on ductility, conduction, and the tensile strength of the samples. The purpose of fabricating conductive composites is to offer counter measures for electrical equipment, which is heavy, bulky, and impractical to use to supress, or reduce the level of EMI. The bio-compostable ingredients used in this research is a new way to combine bio-compostable ingredients with insulative resin

(epoxy), and superlative conductive synthetic graphite, which is not written about in literature. These ingredients are Calcium Lactate, Agar, and Sodium Alginate.

1.2 Motivation and Research Objectives

The main aim of this research is to study the electrical resistance of nanocomposites. This thesis aims to report on size and grade hybrid systems of xGnP in an epoxy blend mix to provide electromagnetic interference shielding through the study of the conductance of the samples made. Mechanical behaviours of the labour-intensive manufactured specimens will be compared using destructive and non-destructive testing, to obtain information regarding tenacity and the island-island interfacial interactions between the platelets. Results will then be calibrated against commercially available resistors; ultra-high precision z-foil resistors. The successful production of high conductance composites would mean not an attenuation but an elimination of EMI.

The objectives of this research are:

1. To study the effects of graphene, and graphite on the composites made relating to volume and size of platelets on electrical conductivity or inversely, resistance.

2. To study the effects of heat, degassing, and mixing methods on the alignment of SG and xGnP platelets, with reference to platelet vacancies in composites. Platelet vacancies are the empty spaces where SG or xGnP platelets are absent within the morphology of the composites, this is more likely to occur in agglomerated sites with less uniform dispersion.

3. To study the tensile strength, and mechanical properties of the nanocomposites.

4. To study the morphology of xGnP and SG nanocomposites.

5. Study the impact of a longer, and leaner processing practice to preserve the platelet morphology (shape and size of the nano-platelets), using lower energy and speed in manufacturing.

1.3 Organisation of the Thesis

Chapter 1 communicates a brief introduction of the background of this research, inclusive of aims and objectives, finishing with the structure of the thesis.

Chapter 2 provides a literature review on the methods used to counter EMI, in addition, the current application of graphene related materials in EMI shielding. It starts with an introduction to the electromagnetic spectrum, then delves into technical definitions of EMI. Later in this chapter, a comparison of intercalation mixing versus mechanical exfoliation is analysed and discussed. The pros and cons of composites are outlined, specifically to labour intensive composites. Other EMIS materials are discussed, as to how they compare to graphene based shielding materials.

Chapter 3 discusses the methodology used for each composite manufacturing process including the details of the materials used. A summarised science background on the used epoxy molecular structure is given, and a detailed standard for the tensile composite is provided.

Chapter 4 involves four parts. Commencing with Visual Inspection of Mixtures, secondly Tensile Data Analysis, thirdly Conductivity Results, which is very short,

fourthly Visual Inspection based on Reflectance. Valuable information is provided to analyse and study unique characteristics of the composites, and the nano-platelets.

Chapter 5 presents conclusions and suggestions for future work.

Chapter 2 - Literature Review

2.1 Overview

Electromagnetic Interference (EMI) encompasses and affects all electric related systems and devices (Weik, 1996). Attenuation is the reduction of electromagnetic interference. EMI is caused by the disturbance of the direction and linearity of electromagnetic waves that results in a disruption, obstruction or interruption that degrades the propagation of Electromagnetic Waves (EMW) that forms a signal through the receiver or the intended destination. The more conductive a medium, the higher the levels of EMI that it can attenuate, thus reducing the level of interference and improving immunity.

Nanocomposites are composites containing materials that are inhomogeneous at atomic scale, and homogenous at macroscopic length scales (Milton, 2003). A composite is the combination of a matrix (binder), which can be in liquid or viscous form, together with a filler that could be any shape or size. A simple composite is a cement, made from water (matrix) and cement powder, which can consist of sand and gravel (filler).

The desired occurrence of a homogenous composite at nanoscale is when all the constituents that are combined into a mix are effectively combined together where no clustering or agglomerations of platelets are present. This allows for a situation of conducting interfacial adhesion or a morphology of a conducting network path (He et al., 2017). On the contrary, a heterogeneous composition occurs when there is a non-uniform separation of the constituent ingredients into macro or microscopic layers. Therefore, detailing a lack of effective interfacial adhesion between the utilised

materials. The desired scenario is that the composite substituents have an attraction towards each other to create a conducting path, which lowers the electrical resistance value. Should our nanocomposites be heterogenous at a microscopic scale, they would show a high electrical resistance value, thus a lack of interfacial attraction at an atomic scale: this is where the exfoliated graphene nanoplatelet (xGnP) islands meet, and the current travels through a conductive network path. Should the circumstance occur where the xGnP or the synthetic graphite (SG) are heterogeneous at both micro and macro scale, this would result in a lack of cohesion and will promote flakiness, therefore unstable specimens.

2.2 The Electromagnetic Spectrum (EMS)

A signal is used to convey information through the transmission of an electrical impulse. Longwave refers to electromagnetic wavelengths within the radio frequency spectrum that is lower than the medium frequency MF wavelength, below 300 kHz, these assign to wavelengths that are larger than 1000 metres (Weik, 1996). Medium frequency is situated between 300 kHz to 3000 kHz, and to 3 MHz. Shortwave pertains to frequencies above the MF, i.e., above 3 MHz, constituting wavelengths that are less than100 metres (Pierson, 1993). An electric field is the result of an electric charge such that of an electron, ion or proton in a volume of space or a medium that houses the charge (Weik, 1996). Thus, for our conductive filler containing composites to be successful, they need to transmit an electrical impulse.

Essentially the EMS can be categorised into two components that inhibit a diverse yet categorical range of frequencies. These two narrowed down components are the radio spectrum that is to the left and the optical spectrum to the right of the electromagnetic spectrum. The visible spectrum being the area that is visible to the naked human eye,

is between 10^{14} and 10^{15}. Immediately to the right of the visible spectrum is the

Ultraviolet frequency, while directly to the left is the infrared frequency.
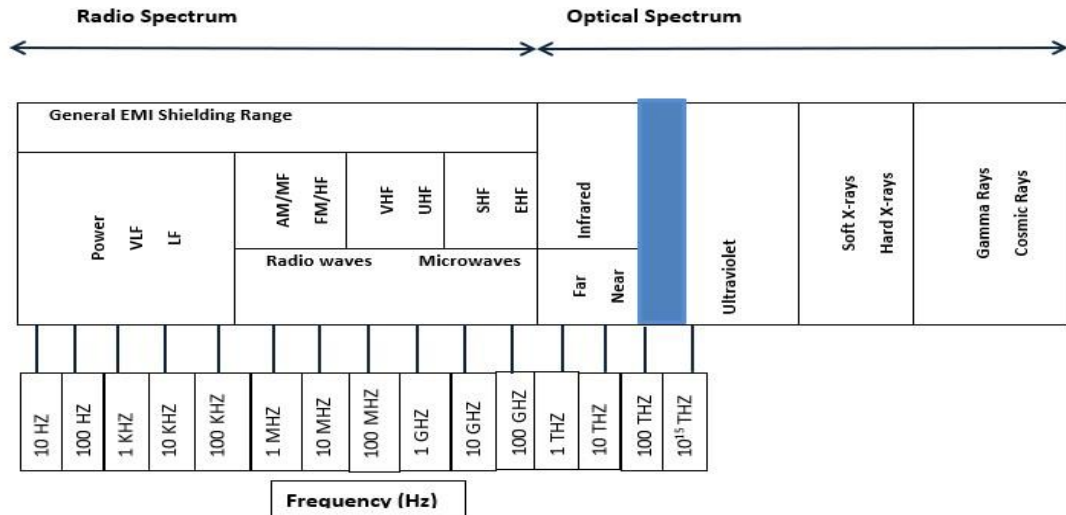
Figure 2-1: The Electromagnetic Spectrum and the general EMI Shielding Range adapted from (Tong, 2009).

The area of concern in this thesis is the radio spectrum; this is where the Electromagnetic Interference Shielding Range exists (Tong, 2009), as seen in figure 2-1. Radio Frequency interference is an interference generated, or that can be induced into an electronic circuit within the radio frequency region in the electromagnetic spectrum. Contrary to this, the EMI is the interference of any electrical noise within the entire electromagnetic spectrum. The main difference is the wave amplitude or frequency. However, telecommunication devices utilise the radio spectrum, whilst other devices such as atomic microscopes use much tighter frequencies such as X-ray diffraction crystallographic at nano scale or other atomic study microscopy.

The radio spectrum consists of wider wavelengths, conversely, the optical spectrum consists of tighter wavelengths. Thus, it possesses tighter amplitudes. Radio

frequency is stated above a frequency within the electromagnetic spectrum; however, it is a frequency that (a) is commonly in association with radio wave propagation and (b) has a frequency range between 3KHz (kilohertz) and 3000 GHz (gigahertz) this amount is adjacent to 3THz (terahertz), (Tong, 2009).

Reducing the specimen's level of susceptibility would mean a high EMI immunity measured. The facility to achieve EMI with effective susceptibility would mean the Electromagnetic Compatibility is achieved. EMI shielding can be accomplished through minimising signals passing through a device or system "either by the reflection of the wave or by absorption and dissipation of the radiation power inside the material" (Wu et al., 2016).

2.3 Definition of EMI and problems caused by EMI

EMI occurs when a device leaks sufficient energy that it adversely impacts the function of another device (Schoen, 2016). EMI is an increasing and consequential form of environmental pollution (Williams, 1995). It exists in the form of crackles during broadcasting transmission, and may result in electric and electronic malfunctions, and can impede the proper usage of the radio frequency spectrum, thus resulting in ignition of flammable or other hazardous environments that may affect the operation of human tissue (Williams, 1995). To reduce EMI copper, aluminium, nickel, steel, and or other metal alloy shielding is applied. This technique of reducing and managing the potential of interference is known as Electromagnetic Compatibility (EMC). Furthermore, graphite and graphene composites are manufactured to provide Electromagnetic Interference Shielding with a multitude of other materials and reinforcements. Some of which combine a few layers graphene with wax to improve the EMI property of paraffin wax, where it was found that few-layer graphene/wax

mixture performed better EMI shielding properties compared to the commercial graphite/wax composites (Song et al., 2013).

Weik (1996) defines EMI as a disturbance caused by electromagnetism that interrupts, obstructs, degrades or limits the performance of electrical equipment, which finds its way into a circuit through coupling, be it conductive, capacitive, or inductive coupling, which can derive from a wide range of sources and frequencies that can be light waves, radio waves, radar pulses, gamma rays, which can endanger the functionality of radio navigation which maybe intentional, i.e., deliberate or unintentional.

Composite EMI shield is an invention patented (US Patent: US2004/0172502), by both Jeff McFadden and Martin Rapp, the applicant being LAIRD TECHNOLOGIES, INC (Justia Patents: 20040020674). It is based on the premise where electrically conductive materials are used as a shield to EMI, whilst energy-absorptive materials are used to suppress EMI. Nanocomposites are composites that involve particle filled polymers consisting of a minimum of one dimension of particles dispersed within a nanometre range (Alexandre et al., 2000) or modulation.

2.3.1 Susceptibility

Susceptibility is the scope or degree to which a device, equipment or a system can be exposed to operative or effective degradation instigated through one or more inherent weaknesses and environmental conditions (Weik, 1996). An example would be the extent to which a communications system can be susceptible to interference via radiant energy that propagates through a field with both magnitude and direction to cause interference from sunspot activity. This radiant energy is also known as radiation which, can be generated from local transmitters or jammers that can cause

electronic warfare, which is different to psychological warfare operations. Electronic warfare is the extent to which electronic equipment can be exposed to electromagnetic radiant energy through hostile forces equipment such as jammers or better known as jamming transmitters/ jamming devices that operate at the same radio frequencies as communications devices such as mobile phones. Susceptibility can be generated intentionally to communications systems with psychological warfare propagation, leaving the subjected target audience with high vulnerability to variant forms of psychological operations.

An electromagnetic wave is the result of time-varying electrical and magnetic fields that exchange energies, causing an interaction of electrical and magnetic energy to propagate towards a direction dependant on the spatial relationship of the interacting fields (Weik, 1996). To conclude, an electromagnetic field propagates without the need for physical support and carries energy, whilst by convention displaying space variation at the matching pace (Pelton et al., 2013).

2.4 Issues resulting from EMI

Sources of Electromagnetic Interference are filterable, containable, and shieldable; are electrical, magnetic, and electromagnetic fields which emanate from wired transmitters, AC power mains, and any system or component that is generated through electricity (Carr, 2000). Fundamental causes of EMI involve:

1) Fundamental Overload,

2) Intermodulation, and

3) Spurious emissions from a transmitter (Carr, 2000).

Fundamental overload is the effect of the affected equipment experiencing an overload via the transmitter's fundamental frequency. The susceptible device or equipment must do either:

    a) Respond to desired signals properly

    b) Not respond to desired signals properly

Fundamental overload requires the equipment not to respond to desired signals properly. This means that the susceptible equipment responds to undesired goals, causing interference, in the realms that the transmitter is legally operated (Carr, 2000).

Intermodulation is the placement of two frequencies in a non-linear motion creating a form of radio interference known as the "rusty bolt effect" of dissimilar metals or conductors that are in contact with each other, hence $mF_1 \mp mF_2$ where m is the integers, and F_1 and F_2 are the frequencies (Carr, 2000).

Transmitter Spurs is when the product of transmitters is a fundamental signal at the operating frequency, in converse transmitters also produce spurious frequencies "spurs", where a licence is absent. These spurs range from harmonics that form the exact integer multiples of the fundamental frequency, noise, parasitic oscillations, harmonics of a local oscillator, mixer products (Carr, 2000).

2.5 Modes of Entry

The way EMI can travel into a device or system in three modes:

    1.   Radiation,

    2.   Conduction, and

3.   Magnetic Induction.

Radiation is where the system is affected by a spur or impulse directly from the antenna. Furthermore, radiation occurs from the direct signals emitted by the antenna through space to the susceptible device.

Conduction happens through wires are connected to the susceptible equipment. Wires include AC power mains, antenna (if included), devices connected to the equipment, and any ground leads.

Magnetic Induction consists of two circuits magnetically coupled, and when a nearby transformer causes interference issues. The level of coupling is determined by the capacitance that is between the emitter and the susceptible device.

Methods of evaluating and locating EMI involve radio frequency sleuthing tools, radio frequency detectors, radio direction finding (RDF), field improvisation, regular loop antennas, sense antenna circuit, switched pattern Radio Frequency antennas, that are all a list of low-cost EMI sensing, evaluating and determination tools (Carr, 2000). To successfully determine where EMI is being transmitted by unambiguous tools are required.

Radio frequency (RF) sleuthing using a portable radio is used to sense a loose power line or to sense the radiation from a malfunctioning electrical system from a nearby building. Radio direction finding RDF by means of locating or radio station or RF noise emitter through a directional electromagnetic wave (EMW) into a radio antenna and receiver. Field improvisation, i.e., using an AM radio. Ultimately a variation of antenna from loopstick to regular loop to direction finding can be used to find unambiguous EMI by the use of cost-effective methods (Carr, 2000).

2.6. Methods to counter EMI and some of their limitations

2.6.1 Electromagnetic Compatibility (EMC)

Electromagnetic Compatibility is the control, and reduction of electromagnetic interference, as it involves the operative design of electrical and electronic systems/components and devices in a systematic process that allows these systems/devices to have higher immunity to the specific amounts of EMI, whilst simultaneously limiting EMI emissions. Electromagnetic shielding is a way to manage interference through the use of electromagnetic compatibility designs in cutting-edge telecommunications equipment, fast processors and digital systems (Tong, 2009).

In contrary, EMI Segregation is the isolation of EMI from the telecommunications signal (Schoen ,2016). Current research observes that to shield against EMI the EMW needs to be reflected and/or absorbed in order to attenuate the undesired signal of EMW leakage (Chen et al., 2016).

The Communications Standards Dictionary (Weik, 1996) describes electromagnetic compatibility (EMC) as the condition that occurs or is existent when the electric component or equipment behaves in the order of its intended functionality and does not experience undesirable or unwanted unintentional EMI resulting from or to other electrical equipment within the same environment. EMC equipment is engineered with design characteristics and features to eliminate and or reject unwanted interference and, in doing so, enhances the operating compatibilities of electromagnetic radiating and receiving components and equipment. Furthermore, EMC equipment is designed for interference free usage determined by the flexibility that is sufficient to enable this. It is also a requirement that EMC equipment is designed within frequency management concepts and doctrines to allow for maximum

operational effectiveness. This includes the ability for operators to deal with interference as and when it should occur if it does, and EMC equipment is designed to function or operate within a specific margin of safety.

Interference: throughout communications, device degradation and the performances of electronic equipment gave birth to the requirement of tools that provide shielding and that block interference. The Michael Faraday cage principle is often used as the technique used to provide shielding. This technique involves the isolation of the susceptible device or medium from outside interference (Schoen, 2016). The way that a Faraday Cage works is that in the most basic way, a foil or conductive mesh surrounds an electrical device (Bradley, 2012) while ensuring that the seams or holes are smaller than the interference wave so that the interference cannot pass through. Then once the EMW that is undesired is propagated towards the surface of the Faraday Cage, one side of the cage becomes positively charged, as the opposite side becomes negatively charged due to charge redistribution. This is the consequence of the electron abundance of the conductive foil or mesh, allowing the redistribution to occur. The cover used, as in the coaxial wire, within the Faraday Cage principle cancel out the external field. The external field and the charge redistribution act as two cancelling components at the conductor surface. Free electrons to the positive ions reflect the undesired EMW that is the interference (Bradley, 2012).
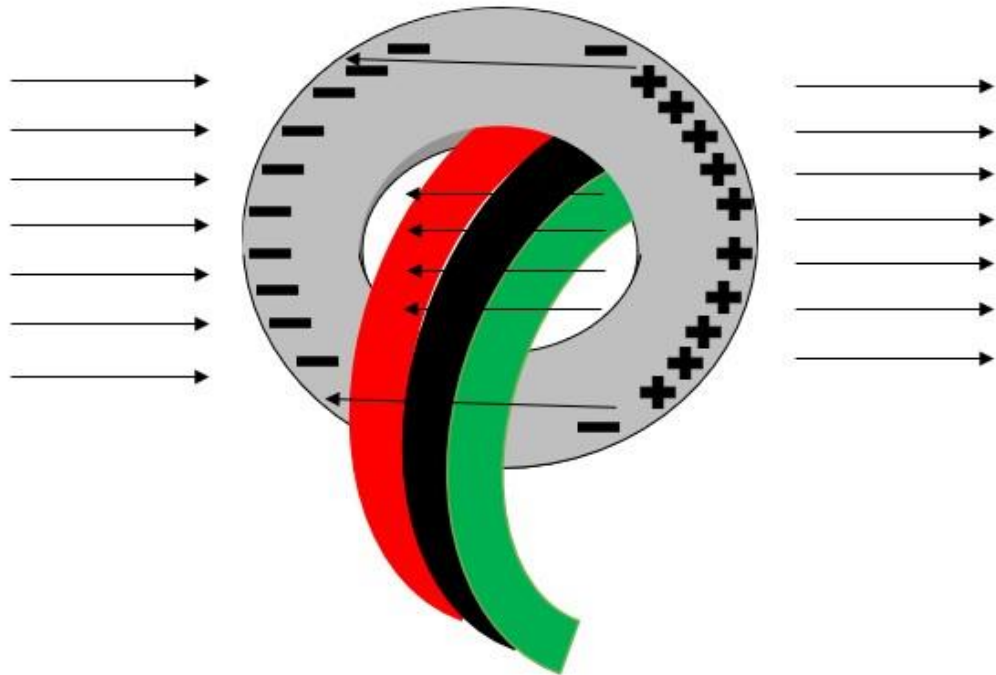
Figure 2-2: The faraday cage field cancellation principle (Bradley, 2012).

The above figure 2-2 shows how electrons redistribute when an electromagnetic field or pulse is induced. The grey circle is the faraday cage of which could be a coaxial wire. This causes the induced pulse to be cancelled by the opposing positive ions, whilst the conductive mesh or foil being the faraday cage provides the protection needed inside, thus cancelling the external field.

2.6.2 Electromagnetic Interference Shielding Effectiveness (EMISE)

Shielding is the means of utilising conductive mediums as shields to reflect and minimize the undesirable effects of sources originating from outside the circuits that contaminate the intended use of the originating circuit. The sources that propagate these interfering, effecting impulses are electromagnetic, electric and magnetic fields. Shields such as that of co-axial wires are used to prevent electromagnetic and electrical fields used in electronic circuits from escaping by means such as dissipation. Insulators are used to create shields by means of protection from hazardous voltage levels, and to provide the simulation of the concept of the Michael

Faraday Cage Principle, explained as providing a shield or cover between the field source and point of receiver, thus reflecting the interference by cancellation.

Shielding effectiveness is in effect a measure to provide for attenuation of EMW, electric, or electromagnetic field strength as a result of the insertion of a shield along or between the field source or also known as the field emitter and the point of measurement. It is the Electromagnetic occurrences that degrade the performance of systems such as a radio receiver directly or indirectly (Weik, 1996).

To create a medium that provides electromagnetic interference shielding effectiveness, it must meet the conductivity threshold of at least 10^2 S/m as outlined by (Kumar et al., 2017).

American Society for Testing Materials ASTM International Standard Test Method for Electromagnetic Shielding Effectiveness of Durable Rigid Wall Relocatable Structures E1851- 15 define the necessary regulated set of guidelines to measure EMISE, whilst on the contrary, EMIS is not primarily focused on the set of standardised regulative methods for shielding effectiveness testing which means that manufacturing smaller composites is a viable option, as with E1851-15 standard requires much a bigger blend mix, and moulds for a cure that are metres in size. For this reason, this research will conduct specimens with 25mm gauge length for practical use of initial research. EMI is an assigned behaviour that occurs to the propagated radio wave at a given frequency, is interrupted, degraded, obstructed or finally limits the wave or signal propagation within the composed medium which can be a composite or any other electric or electronic device. As outlined earlier, EMC is the countermeasure to EMI that is encapsulated within the design of the manufactured electric and electronic medium communicating to constituent devices/systems.

2.7 Immunity

This is the rate of the capacity at which the equipment can withstand the undesired signal from a transmitter culprit. This is useful as it is a mechanism and key term which helps to understand the level of EMC within the measured component or device. Furthermore, it would be a very clear distinction between the ability of our composites to inhibit EMI or to show shielding capabilities. An EMI culprit is one where the interference is radiated from, whilst an EMI victim is the device that receives the undesired or unwanted interference.

2.8 Current application of graphene related materials in EMI shielding

Oxidised graphene is used for radar absorbing material (RAM) that is designed with features to provide electromagnetic shielding (EMS). In addition, EMS materials are required in the rapid growth within the following industries: satellite, electronic, and telecommunications, specifically within the GHz frequency range Acharya and Datar (2020). The total shielding effectiveness value is defined by Acharya and Datar (2020) as the amalgamation of shielding effectiveness caused by reflection and adsorption. The latter reference report that shielding effectiveness of more than 90% has been achieved in the ~60 dB X band as well as ~50 dB in the Ku band. Whilst EMI reflection-based materials reflect the interference, the advantage of absorption-based materials is that the EMI is decayed, whereby absorption does not create another source of electromagnetic waves as what could happen with reflection. Historically, reflection materials tend to be metals that are impractical and heavy, and so research has been directed towards composites. Impedance matching of the electromagnetic waves determines whether absorption or reflection of interference has occurred. When a mismatch of impedance, this means that electromagnetic waves are reflected. However, if a maximum match of impedance happens where the electromagnetic waves enter the

medium through means of free electrons and dipole moments, then the energy of the electromagnetic wave is then dissipated, which means that the waves are not reflected back or transmitted. For this situation to occur, a perfect amalgamation of complex permittivity, permeability, conductivity relative to the thickness of the intended shielding material is required Acharya and Datar (2020). This last-mentioned reference also reports that to obtain excellent radar absorbing material then a combination of magnetic as well as conducting material is needed. In contrast, if the composite contains a conducting graphene material percentage is higher, then this can lead to the likelihood of the shielding efficiency (SE) to be dominated by reflection in SE. To get around this, the absorption shielding capacity needs to be increased. One of the ways to do this is to add a component with magnetic properties, which would create a hybrid structure of graphene and magnetic ferrite composite. Other applications of graphene related materials specific to GnP were manufactured due to the need for strategic systems used in aircrafts, nuclear reactors, communication systems, transformers and control systems that require these materials to shield against EMI (Geetha et al., 2009). It is documented within research that there are some outstanding issues within the structural and cellular morphology, which were affected, thus limiting the percolation of the graphene networks (Geetha et al., 2009).

2.8.1 Carbonaceous Filler

The inclusion of carbon nano-reinforcements such as xGnP improves the efficiency of stress transfer within the reinforcement polymer interface (Kim et al., 2010). Other factors of the reinforcement, such as shape, aspect ratio, orientation, dispersion, and distribution will affect the reinforcing efficiency of the reinforcement (Kim et al., 2010). These latter factors will also affect the ease at which electricity will flow through the fabricated specimens. Graphene is one atomic layer of graphite, and

graphite is made of many layers of graphene. One atom thick sheets of carbon as a layered material make up the carbonaceous carbon allotrope that is graphite. These carbon atoms are covalently bonded together in a hexagonal arrangement constituting a layer, and these layers are bonded to one another by weak van der waals forces. Within literature, it has been reported that adding a reinforcement with an adequate rate of aspect ratio can significantly enhance the mechanical properties of the composite material (He et al., 2017).

In order for electricity to travel through composites, the electron tunnelling theory determines that an electron is dependent on the magnitude or ability of electricity to travel, infiltrate, or penetrate across the potential of a barrier, as long as the energy radiated is larger than the potential barrier (Max Planck Institute, 2018). So, to bring the latter two points of the aspect ratio and the electron tunnelling theory, our composites would need to be optimal for the interfacial interactions of the xGnP platelets with each other, within and between their localities, being between and within each other, enough to create a percolation threshold to enable the generation of electrical conductance. Electricity takes the shortest route; electron tunnelling theory depends on the magnitude of the electron to pass through the barrier of island-island interfacial connectivity. Therefore, our composites need to allow the electric field to penetrate through this resistive barrier of platelet misalignment and become conductive by eliminating vacancy holes. When platelets are aligned in a way to channel the electrons, the potential for electricity to pass through our mediums/ composites may be greater.

2.8.2 Epoxy

The chemistry and properties of epoxy resins will be studied here; they were first commercially used in 1946 due to their ability to limit by-product processes and, their adaptability to undergo small levels of shrinking (Garnish, 1972).

Polymers have gathered a reputation for their high specific strength and flexibility, yet they can (inclusive of rubbers and thermoset resins) have either low absolute strength or poor fracture toughness, thus limiting their viability across industry applications (Zaman et al., 2011). To overcome this obstacle, polymers are combined with a variety of fillers, including carbonaceous fillers such as GNP, carbon black and carbon nanotubes. However, single walled carbon nanotubes portray high viscosity conveyed by the "bird's nest" structure of the entanglement of nanotubes that persists into anisotropy functionality. Whilst GNP, are more abundant in nature, generating a cost-effective material combined with their extremely high surface area, which allows for a more uniform or a higher level of stress transfer across the medium interface. Thus, providing a sturdier reinforcement (Zaman et al., 2011). Essentially epoxy resins are a categorical group of polymers that contain, in this case, two epoxide groups terminally at the molecular structure that can then be turned into thermosetting plastics with the addition of corresponding curing agents (Hameed et al., 2017). This class of resins (epoxy) have been put into use for a wide range of specifics, some of which are coatings, adhesives, electrical insulators, electronics encapsulation materials, casting compounds for prototype moulds, caulking and sealants, impregnation of resins, floor topping, and printing inks (Lee et al., 1967, and Hameed et al., 2017). They have also been of vital importance in matrices of fibrous components due to their characteristics of having excellent adhesiveness, chemical resistance in conjunction with their mechanical and physical properties (ASTM

International D638, 2014). Due to the highly cross-linked three-dimensional network structure of epoxy resins, cured epoxy results in a generally improved stiffness, strength, creep resistance, heat resistance (Gui et al., 2014). They also obtain solvent barrier properties in assessment to thermoplastic polymers that can be reheated and remoulded after the initial cure (Gui et al., 2014).

However, the generic characteristic of epoxy resins is that they are inherently brittle, which makes them prone to micro-cracks, therefore limiting their applications (Hameed et al., 2017). To combat this, researchers combine the epoxy polymer with a toughener that adds some of the desirable properties, i.e., fracture toughness (Hameed et al., 2017). This is achieved through the addition of second-phase polymeric particles known as rubber toughened epoxy. Some of the factors that influence the toughening effect relative to the later point of rubber toughened epoxy include rubber make-up, particle size and the matrix characteristics (Hameed et al., 2017).

Epoxy resins are utilised in a wide range of industries; however they are disputed due to their incomprehensible nature to be melted and be reformed. However, they exhibit resistance to chemical attack, with high adhesive strength and environmental resistivity (Garnish, 1972). It is the effects of a three membered ring known as the epoxide group opening that generates the crosslinking of the substituents and solidify, i.e. cure, the process of the chemical reaction through solidification group epoxides as thermoset resins. The epoxide composition composes of a minimum of two constituents, the resin and hardener, satisfying curing. Modification of cure properties and assisting processing constituents used are fillers, dyes, solvents, dilutants, accelerators and plasticizers (Garnish, 1972). The epoxy resin utilised in this thesis are prepared by means of dehydrohalogenation, whereby the elimination of a

hydrogen atom of an intermediate is prepared by the reaction of epichlorohydrin

consisting of a hydrogen containing molecule (Garnish, 1972).
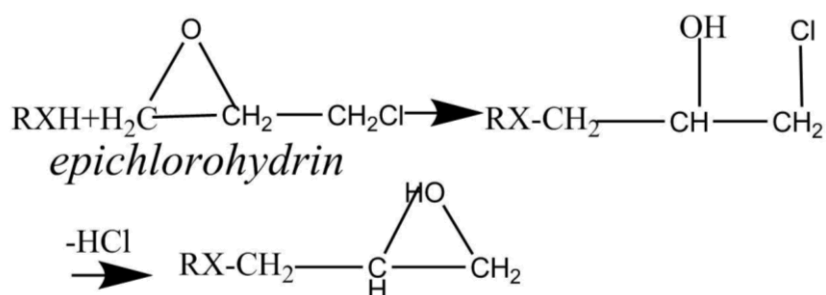
Figure 2-3: Molecular structure of epichlorohydrin, (Garnish, 1972).

The above molecular structure of epichlorohydrin in figure 2-3 shows an overall

molecular structure of the molecular groups within the epoxy resin used in this

research. The terminal ending epoxide ring is what causes the cure between the resin

and hardener.

Resin manufacture: The commercial items used in epoxy being bisphenol A and

epichlorohydrin, condensed together, at modestly elevated temperatures. Within this

mix are alkali constituents that catalyse to produce the chlorohydrin intermediate and

perform as dehydrohalogenating agent that react to eliminate hydrochloric acid. Two

terminally ending epichlorohydrin molecules are required to satisfy the diepoxide,

otherwise known as the epoxide ring.
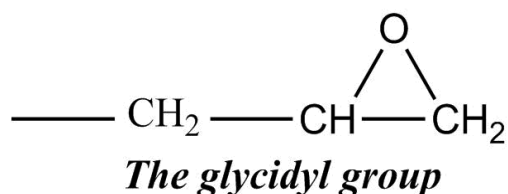
Figure 2-4: Molecular structure of the glycidyl group (Garnish, 1972).

The terminal group inclusive of the epoxide ring, as seen in figure 2-4, is known as

the gylcidyl group, and the general formula of resins can be called polyglycidyl ethers

(Garnish, 2917). The pure form of this compound is known as the crystalline compound. The molecular weight is attributed to the number of repeats of DGEBA, and as the number of this increases, in contrast, the number of epoxide groups decreases, including the hydroxyl groups. The epoxy production varies from low to high viscosity liquids, to soft, and finally relatively brittle solids (Garnish, 1972). The epoxide ring is susceptible to attack and is strained from a range of substances consisting of hydrogen atoms, be it primary and secondary amines, amides, acids, acid anhydrides and thiols. In homo-polymerisation, epoxide groups react with each other and then catalyse using acids, such as Lewis acids or bases like tertiary amines (Garnish, 1972).

The series of crosslinking reactions are as follows. Initially, the reactivity of the general resin formula is dependent on the presence of hydroxyl groups, then step (1a) and (1b) feature ester making processing and reactivity (2) favourably at high temperatures is the action of homo-polymerisation. Both numeral steps create the ideal scenario for the continuation of hydroxyl group generation. Utilising anhydrides with accelerators can speed the cure reactivity. Tertiary amines help in opening the anhydride ring and so encourage the esterification reaction (Garnish, 1972) and special polymerisation processes. The solution is to increase the amount of anhydride within mixtures.

Due to the variant nature of the mechanical properties of polymers and their composites, anomalies of strain studies are conducted. However, studies to assess the medium strain are not well established (Gurusideswar et al., 2017). In this study, low strain techniques using conventional servo-hydraulic machines are carried out for testing, because of the inertial effects of the grips and load cell assembly are confined to lower strain rates <10 s $^{-1}$ (Gurusideswar et al., 2017).

2.8.3 Graphene Sp^2 hybrid orbital (Mechanical, characteristic, properties)

Graphene is often reported as 200 times stronger than steel and is simultaneously extremely lightweight and durable. Graphene is electrically, thermally conductive yet is also transparent at one single atomic layer and is the world's first 2D material. Graphene is an allotrope of carbon at one atom thickness whilst having a two-dimensional honeycomb lattice nanostructure. Some of graphene's wonder properties, such as its Sp^2 hybridised atomic orbital, mean that graphene has a planar structure, forming the commonly known honeycomb carbon hexagon shape. This may mean that the alignment of the nanoplatelets may be feasible, however, this requires research into the manipulation of the gradual platelet alignment. This research sets out to study the behaviour of platelets under a variation of heat and mixing methods. Thus, the graphene nanoplatelets utilised within this research are hexagonal in shape platelets at differing aspect ratios and differing surface area sizes, which are widely contrasted. The objective of this research is to see whether combining a variation in nano-platelet size affects the challenge of achieving conduction at a low percolation theory, which may encourage the conductivity of the xGnP within the insulating resin. Therefore, maximising the rate of filler cohesion and dispersion throughout the nanocomposite. Graphene has attracted attention since its inception by Kostya S. Novoselov and Andre K. Geim at the University of Manchester in 2004 due to its versatile applications within nanotechnology fields such as that of electronics, energy storage (supercapacitors), semiconductor and medical applications within biomedicine (Jiaming et al., 2016).

2.8.4 Synthetic Graphite

Synthetic Graphite is manufactured using calcined delayed coking, and the needle-coke is most valuable (Ragan et al., 1983). To manufacture synthetic graphite, a series

of rotary kilns, rotary hearths, and vertical shafters are techniques that are utilised to produce SG in an anomaly of outputs (Ragan et al., 1983). The seven main stages of the manufacturing process of SG, as outlined by the last discussed reference are: mixing, forming, extrusion, moulding, baking, impregnation, and graphitisation. Depending on the source of material, condition and techniques of SG manufacture can vary largely in density, electrical resistivity, mechanical strength, porosity, and optical texture (Ragan et al., 1983). Thus, purposes of use and detail specification controls are variable. SG, among other ingredients, contain predominantly petroleum filler, and coal tar which are combined through mixing, and the final shape is dictated through moulding or extrusion and finally graphitisation. As supported by Ragan et al., graphitisation is a heat treatment of the baked artefact to 3300K (Ragan et al., 1983). This treatment of electrical heat to the baked SG, in this case, causes the carbon atoms to move into a thermodynamically high increase of stable graphite lattice (Ragan et al., 1983).

Anwar et al. (2016) state that graphite is an anisotropic material having fine thermal conductance and electrical properties within their "Recent Developments in Epoxy/Graphite" paper. This latter paper also discusses the property of graphite ability to conduct electricity. Thus it is utilised for brushes used in electric motors (influenced by the in-plane covalent bonding) and electrochemical electrodes that are driven perpendicular to layers. As the carbon layers can slide over each other, this means that graphite is good as a lubricant material and in some forms of pencils (Anwar et al., 2016). Cubberly (1988) defines anisotropy as exhibiting different properties when characteristics of strength or coefficients of thermal expansion, for instance, in different directions with respect to a given reference, such as a specific

lattice direction in a crystalline substance owing to anisotropy, to exist in graphene layers (Anwar et al., 2016).

It is important to note that graphite's inherent property is that it has directional thermal conductivity, higher conductance in the basal plane (Pierson,1993). Furthermore, Pierson quotes it is possible to consider graphite as a semi-metal; the highest filled valence band covers partly the lowest-empty conduction band by approximation of 36 MeV. The fourth valence shell is partly filled with electrons that form a partially filled conduction band at which the electrons move in a wave form between the basal planes in response to electric fields (Pierson, 1993).

2.9 Other EMIS materials and how they compare to graphene based shielding materials

Spinel ferrite nanoparticles are combined with a polymer for EMIS applications (Yadav et al., 2020). Spinel ferrite nanoparticles physical properties are determined partly by their particle size, defects, interfaces, and morphology. This is similar to the properties of xGnP platelets whereby composition, and alignment of the nano-platelet, combined with those listed for spinel ferrite, determine whether electricity can travel through an epoxy xGnP composite. Yadav et al. found that the effectiveness of spinel ferrite for shielding applications depends on the preparation method, synthesis conditions and their mixing with organic or inorganic matter (Yadav et al., 2020).

Other materials used for EMIS applications involve carbon fillers such as carbon black, carbon fibre, carbon nanotubes and graphene that are dispersed into a polymer matrix by means of melt-blending and solution processing (Thomassin et al., 2013).

This latter paper finds that using cheap carbon filler often requires a very high percentage of filler, which undesirably can hinder other material/composite properties. This is also a problem that is evident with graphene filler (Kumar et al., 2017). Bailly et al. reported that in order for the composites to be conductive and or have a high dielectric constant (the ability to store electricity), the carbon particles need to have an established 3D network with contact between the particles bearing closeness (Bailly et al., 2013). They also found that the aspect ratio of the differing carbon filler is a key parameter to conductance, with graphene sheet having the highest conductance, followed by carbon nanotube and least conductance being carbon black. They also report that the dispersion technique is another important parameter, which the high aspect ratio of the fillers needs to be preserved. This will be the intention of this research to disperse and combine the blend mix whilst maintaining the integral structure of the nanoplatelets through a combination of intercalation and mechanical exfoliation.

2.10 The reason for Composites

Whilst composites are not the same as nanocomposites, it is useful to cover some basic aspects of the advantages of nanocomposites, as in this research, nanoparticles are being used as filler. Drzal outlined that nanocomposites exhibit property enhancement such as the mass reduction of density and thus a low concentration, a progressively improved appearance of scratch and mar resistance, improved electrical conductivity inclusive of electrostatic dissipation, and electromagnetic shielding. Other enhanced properties also include thermal conductivity and barrier to permeants (platelets) (Drzal 2006).

It is found in research publications that epoxy property improvement (mechanical, thermal, electrical) can be exhibited at low filler loading (Anwar et al., 2016). Furthermore, extensive progress in mechanical, electrical, and thermal properties has been observed in epoxy composites that are reinforced with graphite, graphene, and GNPS (Anwar et al., 2016).

In polymer matrices, the degree of dispersion of pure graphene is extremely poor (Anwar et al., 2016). Polymer/graphene nanocomposite can be applied using surface-modified graphene, which would then be dispersed into an organic polymer matrix such as epoxy (Anwar et al., 2016). Then the visually dispersed epoxy/graphene nanocomposite should exhibit improved mechanical, thermal, but not always electrical, and some gas barrier properties with a suitable distribution of graphene in the matrix (Anwar et al., 2016).

The polar interaction between GNP and epoxy matrix might be accountable for better filler dispersion and improved epoxy/GNP properties (Anwar et al., 2016).

2.11 Manufacturing of composites containing graphene/ graphite related materials

Ren et al. researched three forms of moulding method 1) melt extrusion followed by injection moulding, 2) single injection moulding, and 3) hot-pressing (Ren et al., 2019). They had found that the moulding methods had no effects on the crystallinity and the constitution or composition of the composites.

Jun et al. found that by compounding, mechanical stirring for better dispersion, using a vacuum oven to dry ingredients, followed by pelletising and desiccating at 60°C for 12 hours, at least twice to remove moisture and finally drying and pelletising the ingredients before putting through an injection mould machine, improved thermal

stability as the GnP amount increase for all grades experimented including H1100, C300, M5 and M25 (Jun et al., 2018). The urgency for EMIS is growing ever more in demand due to the rise of fast processors and miniaturized mobile technological advances. Traditionally metal resources have been used predominantly for systems/components, but since the inception of electrically conductive polymer composites, metals are associated with being expensive, heavy, bulky, and prone to oxidation or better known as corrosion. Light-weight polymeric mediums are favoured and have received significant interest due to their flexibility in geometric composition specific to a size relative to the manufacture of a high surface to strength ratio. Composites have a very low density, and they are able to sustain chemical corrosion. However, some inconveniently exhibit insulative behaviours (Kumar et al., 2017).

Epoxies are used as a matrix due to their high performance in composites. Some of their excellent qualities include processing versatility, thus the ability to be processed in the use of hand-layup. Another feature in which they excel is that they have low shrinkage. Therefore, they can mould into a given cavity with retained dimensional stability. Other features include excellence in strength and adhesion (Campbell Jr, 2003). A problematic result of high viscosity that is created through the overwhelming use of the nanoparticles would mean high levels of groups of agglomeration of the nanoparticles would be present (Kuester et al., 2017). This results in a brittle composite with low toughness qualities. In general, epoxy resin can lead to short cycle time, low volatile emissions and provides high quality components.

The versatility of epoxy handle allows for the nanocomposites to be created through a labour-intensive process. It can be manoeuvred without the need for the mix to be subjected to pressure or heat in order for the epoxy to cure. It is described that when

comparing nanocomposites to traditional composites, nanocomposites display "extraordinary properties" due to the high surface to volume ratio of the nanofillers, whilst including the features of the high aspect ratio (Zaman et al., 2011). This gives greater agility to control and manage each stage of manufacture, as the epoxy composite tendencies can be predetermined by the use of a labour-intensive layup.

Sevkat and Brahimi (2011) found that the geometrical parameters of the hand-lay-up process produced very effective technical properties of bearing load, progression on failure modes, and magnitude sustained load. Sevkat & Brahimi (2011) discuss a variation of disadvantages of utilising the hand layup process, some of which are listed below.

1. The process is labour intensive that can cause high cycle times in manufacturing processes, with low production scale and output volumes.

2. The hand-lay-up in its nature can produce inconsistent structure orientations and can also cause variable thickness in composites.

   This problem is difficult to resolve, as using a scraping tool that is almost like a squeegee, which will glide past the surface of the blend mix and avoid scraping blend mix that is required to create a sample, in actual fact damages the suspension of the blend mix. However, this may be rearranged during curing, causing added air within specimens.

3. The problem of variable thickness can be a major disadvantage "because its dimensional tolerances often yield composites of non-uniform fibre volume and mechanical strength".

In contrast, Sevkat & Brahimi (2011) discuss the advantages of the hand layup process to be as outlined below.

1. That hand layup attributes of low-cost manufacture of complex composites.

2. That the hand layup process allows the ability to fabricate complex parts, with a reasonably fast initial start-up.

3. That the hand layup process enables the use of easily understood equipment and tooling that require reduced expenses comparably to other manufacturing processes.

In addition, Hörold (1999) contributes to the argument around the disadvantages of hand lay-up is that the quantity of filler used is limited due to viscosity issues, so this is one possible downside to this way of manufacture as opposed to other manufacturing processes such as compression or injection moulding, where the use of high viscosity liquid composite moulding is viable. However, the use of low viscosity blend mix would mean an ease in mass transportation application. This usually means a low-density composite.

According to Patent No.: US8,648,132 B2 (Nanocomposite method of manufacture), declares that the diameter of a nanoparticle is less than 500nm, whilst delivering advantages like that of reinforcement, flame retardant, and providing equivocal or superior or an improvement on mechanical performance (US Patents: US8,648,132 B2), in comparison to the case of the polymer or filler separately. In this case, the xGnP is the monomer nano-filler, whilst the epoxy resin/hardener is the polymer ingredient. The epoxy resin is a thermoset polymer, which means that it cures under heat and pressure, and once solidified, cannot be softened and remoulded, which is a

trait of epoxies (Morena, 1997), known as a thermoset polymer. GNP is defined as nanoparticles consisting of short stacks shaped platelets of graphene sheet that match that found with carbon nanotube walls, however in planar form. GNP is utilised in this research for its well-reviewed ability to enhance chemical and thermal stability and electrical conductivity (Tokala et al., 2015). It is documented that with the inclusion of GNP the mechanical characteristics of nanocomposites are enhanced due to the "unique nanoscale structure, morphology and, composition" (Tokala et al., 2015). It is outlined that by adding "extremely small" loads of graphene, the physical properties of epoxy can be significantly increased (Zaman et al., 2011).

2.11.1 Mechanical exfoliation of graphite/graphene during composite manufacture

Exfoliated Graphite Nanoplatelets are platelets that have undergone exfoliation of graphite, turning graphite into graphene using ionic gases before being supplied and processed into composites. They were required due to their level of carbon purity of over 98% and geometries. A standard overhead mechanical stirrer does provide mechanical exfoliation, but the technology of the stirrer used along with the shape of the exfoliation tool will result in the level of dispersion of the nanoparticles or platelets to be less uniform and result in a lower level of dispersion. A high shear mixer as the ones provided by the company Silverson Ltd are shear mixers with up to 5000 RPM and are provided with a variety of exfoliation tools. Silverson Ltd. advises that for the nanoparticles used (graphite and graphene), the suitable exfoliation tool is a square hole shear mixer tool. However, in this research, a standard electric mixer will be utilised at a fairly low RPM no more than 1300RPM to manipulate and reduce breakage of the morphology of the nanoplatelets visually and microscopically during the processing of manufacture, so that the platelets lay more uniformly in the Ab

plane. Though, using a standard electric mixer would mean a greater probability of nanoparticle agglomerations and groupings of platelets. This is because a much lower level of nano-platelet exfoliation is being achieved.

In order to obtain a high dispersity of the xGnP, SG fillers are required to be subjected to a high level of exfoliation using a high shear mixer. However, this can compromise the morphology of the graphite fillers. A high level of mechanical exfoliation can result in lower levels of agglomerations, but they can, on the contrary, cause the graphite filler to break and degrade in shape. Drzal (2006) outlined that xGnP is a layered natural mineral whose layers can be intercalated with alkalis, acids, and salts to obtain nano size platelets having a high aspect ratio. The sheets and layers of graphite and xGnP are exfoliated and intercalated simultaneously. The edges of the xGnP are functional, and hydrogen or covalent bonds can be activated within a polymer matrix (Drzal, 2006). The latter reference adds that the combination of polymer and xGnP tends to lead to improved electrical, mechanical, thermal, and barrier properties of composites.

The minimum percolation threshold for conductive fillers is 15%, and the minimum electrical conductance of our specimens is 10^{-8} to 10^6 Siemens per metre to enable their commercial viability and for ease in processing and tunable electrical properties (Kumar et al., 2017). However, polymers that depict a low conductivity (from 10^{-10} to 10^{-5} S/ cm) are neutral in respect to conductance, and this property can be improved by a measure of up 10^4 Siemens per cm. However, the means by which this happens is unclear.

The below figure 2-5 depicts the intercalation versus the exfoliation process to produce NanoPlatelet Reinforced-Polymer Composites.
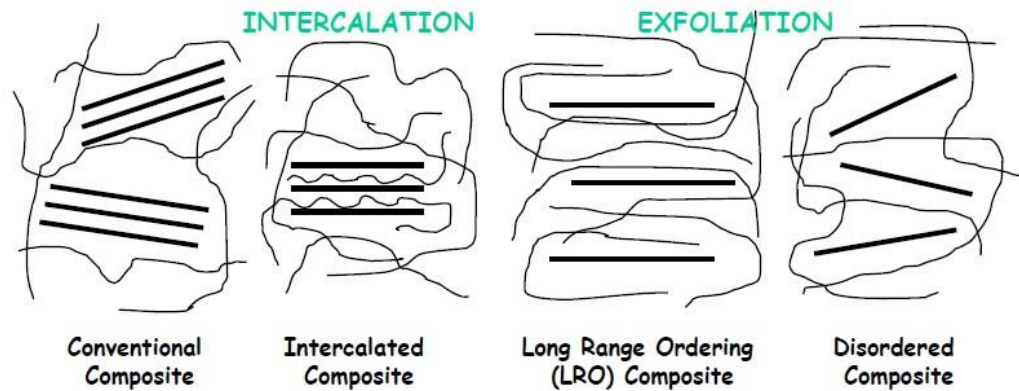
Figure 2-5: Image of nanoplatelet composite composition, sourced from lecture handout (Drzal, 2006).

2.11.2 Intercalation versus Mechanical Exfoliation

This is the study of the manufacture of graphene and graphite composites comparing the previously discussed mechanical exfoliation, which can be by use of high shear mixing or intercalation (above), to which this research utilises the use of a magnetic stirrer and sonicator for achieving a more intercalated composite. Intercalation is when the blend mix is mixed in a different way, which results in the layering of the filler and matrix. To perform intercalation, a magnetic stirrer and a sonicator are to be used in this research for intercalation, whilst for exfoliation processing, a mechanical stirrer is to be used. The aim of intercalation is to get the platelets to align in a linear way to stop the clustering of platelets to achieve better dispersibility layer by layer. However, in this research, a combination of exfoliation and intercalation was carried out with the aim to manipulate the platelet axis. Using a high shear mixer for exfoliation does provide better dispersion. However, the natural or original shape of the platelets may be compromised due to the high levels of RPM and the exfoliation tooling used. So, the intention here is to try to obtain the optimum of dispersion using a combination of low RPM exfoliation and intercalation processes using a longer

duration manufacturing process. During exfoliation, the layers are dispersed in a multitude of platelet axis, whilst intercalation uses a mechanism to subside the platelets with the insertion of the matrix layer by layer, as seen in the above figure 2-5.

2.11.3 Intercalated graphite compounds IGC

Intercalated graphite compounds are created when a non-graphite (foreign) species, i.e., the resin is inserted between the graphite lattice layers, to manufacture a superlative specimen or, in this case, a composite that allows the conductive graphite to be utilised as a conductive medium for conductive devices in a cured resin. The term intercalated compounds come from the simple insertion of a foreign species in between graphite layers, thus creating graphite compounds. The non-graphite species can take the form of atoms, ions, or molecules. Pierson (1993) identified that intercalated graphite compounds could take form in two general classes with varying characteristics, those being (a) covalent compounds and (b) intercalation compounds. Pierson (1993) describes that covalent graphite compounds contain two electron bonds that are situated between the foreign species and the carbon atoms. These two electron bonds disturb the bonds between the layers. Pierson also describes that the interlayer spacing increases with the insertion of the foreign media. Similarly, graphite intercalation compounds take form by the insertion of foreign material into the graphite lattice. However, the difference between the two general classes is that, as with graphite intercalation compounds, the type of bonding is that of a charge transfer, whilst covalent graphite compounds involve covalent bonding. The charge transfer causes an electronic interaction, therefore increasing the electrical conductivity of graphite in the ab plane angle direction. On combining the host with

foreign material, intercalation compounds display a vast spread of graphite composition as the percentage of intercalation increases (Pierson, 1993). The first-stage compound (as shown in Figure 2-6) means that the intercalation is at its maximum and is therefore stoichiometric. IGC can be exfoliated upon the heating of graphene (Anwar et al., 2016). This reference also describes that in graphite intercalated compounds, GIC "charge is transferred between graphite and intercalates leading to greater electrical conductivity than in non-intercalated graphite compounds". Thus, this rate of conductivity facilitates higher shielding efficiency against EMI.
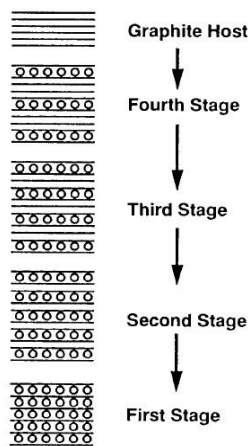
Figure 2-6: The four stages of the graphite intercalation compound Pierson (1993).

The above figure 2-6 is a possible example of SG, xGnP alignment through mechanical exfoliation and heat treatment. Pierson (1993) explains that this is the intended product of intercalation compound processing of graphite.

Graphene and graphene nanoplatelets are recently developed carbon nanomaterials. This form of nanomaterials is comprised of short stacks of specification varied

graphite layers known as graphene that increases the tensile modulus of a composite (Anwar et al., 2016).

2.12 Compostable food grade ingredients to influence ductility

Researchers have shown that using agar in composites with neat poly(butylene adipate-co-terephatalate) (PBAT) shows ductile behaviour (Madera-Santana et al., 2009). They used injection moulding and extrusion to manufacture their biodegradable composites. Furthermore, they show that by adding agar, the stress/strain curve was affected. At 10% agar, results showed greater yield and strain, whilst at 30% and 40%, the stress/strain curve displayed lower strain, thus less yield. Sedlarik et al. illustrated that by adding calcium lactate to biocomposites a colour change was caused to turn the colour to whitish (Sedlarik et al., 2009).

2.12.1 Agar

Agar is sourced from a specific species of red seaweed that is processed for the use of gelling agents in a microbiological culture medium, foods, medicines, cosmetic creams, and to form various jellies (Dictionary of Chemistry Oxford, 2016).

Agar is used in petri dishes as a barrier for the bacteria, or the item being studied is cornered into a specific part of the petri dish. Furthermore, agar is documented to have been used in research of biodegradable packaging. However, agar inhibits poor to moderate mechanical strength and thermal stability (Belay., 2017). Not only do these properties create a concern for its use in commercial packaging, but agars poor resistance to water caused the researchers to combine agar with graphene oxide (GO) and reduced graphene oxide (RGO) (Belay et al., 2017). They had found that the tensile strength had improved with both GO and RGO loading. The interfacial

bonding proved to be better with GO. The contact angle being the hydrophobicity and the resistance to swelling proved better results as compared to pure agar. Belay et al. also found that under morphological investigation, the formation of pores was prevalent, which was a contributing factor for the decrease in tensile strength (Belay et al., 2017).

2.12.2 Calcium Lactate

Calcium Lactate is used in composites because of its biocompatibility, biological availability, and its enhanced mechanical and thermal properties (Sedlarik et al.,2009). Calcium Lactate is to b used in this research to see whether the natural moisture of the ingredient would impact the tensile strength of the biocomposite samples and whether the hydroxyl groups within the chemical would enhance the mechanical and thermal properties of the specimens.

It affects the tunnelling of electrical current due to its insulative nature. However, the choice of using calcium lactate with graphene has not been used in graphene-based composites prior to this thesis.

2.12.3 Sodium Alginate

Sodium Alginate is utilised in bio-composites due to its biodegradability and biopolymer properties as an alternative to petroleum products that are non-biodegradable. Sodium Alginate will be used in the research to see whether ductility and biodegradability values would be visible at tensile loading. This may show whether epoxy, a thermoset resin, can be manipulated into thermoplastic softening behaviours. Sodium alginate has been used in research previously for adsorption purposes with lignin and graphene, where the composite was fabricated using hydrothermal polymerisation in an aqueous solution (Zhou et al., 2018). Through

their research, Zhou et al. found the porous graphene/lignin/sodium alginate showed an increase in the adsorption capacity.

Thermosets that inhibit these properties are plastics that are once cured by heat or chemical processes and turned into "infusible and insoluble" mediums or materials (Tomsic, 2000). The process of thermosetting is the curing of resin by heat and will not soften up on the reintroduction of heat. A thermosetting resin or a thermoset is an organic material that solidifies upon heat and is not remoulded, such as the epoxy resin used in this thesis.

Thermoplastic properties are a class of resins that can be readily softened and remoulded through heating. Biodegradability is the characteristic of a material or a substance to be decomposed through the mechanics of microorganisms.

Biocomposites are composites that use a resin as the matrix and reinforcements that are natural fibres. My research that examines the biodegradability of epoxy thermoset plastics utilises a combination of natural reinforcements and synthetic graphite. The results obtained will examine whether manipulation of natural and synthetic ingredients can persuade the stagnant thermoset epoxy to soften.

To overcome everyday problems encountered via EMI. This thesis will assess whether combining GNP at different studied ratios will create a stronger interfacial adhesion of the conductive reinforcement. Thus, creating countermeasures to the undesired high percolation theory that is anticipated to result in an even more brittle nanocomposite. High purity grade graphene will be examined.

To conclude, literature shows that the current standard of research in this area and the gaps of the research in this area with 15% minimum percolation threshold, which compromises the integral strength of epoxy composites, illustrate the need to obtain a

conducting network within the nanocomposites at lower filler weight percentage. Due to this, my research will be using a combination of intercalation and mechanical exfoliation methods combined with a comparison of synthetic graphite and high purity xGnP. This is to find whether manipulation of mixing techniques and a lower percentage of filler can help improve the composition, and the morphology of the nano-platelets, thereby improving the alignment of platelets. In addition, this research will carry out experimentation using biocompostable ingredients alongside synthetic graphite filler to see whether the ductility of the specimens is improved. Finally, the use of calcium lactate combined with epoxy resin and synthetic graphite has not been found in publications prior to this research.

Chapter 3 - Research methods

3.1 Introduction

The method of production utilises a combination of labour-intensive layup and a variety of mixing machinery. Mixing is used for mixing the materials, whilst layup is for making composites. A hand layup manufacturing process was employed due to practicality and the greater control of the initial processing of materials, to gain an understanding of the viscoelasticity of the resin by observation of mechanical behaviour through physical, labour mixing of hardener, and layup of composite.

3.2 Materials

3.2.1 Filler

There are two types of conductive filler used in this research. The higher purity filler being exfoliated graphene nanoplatelets at two classes M25, and C750. The other conductive filler being synthetic graphite. Other bio-compostable fillers used are agar, calcium lactate, and sodium alginate.

3.2.2 Exfoliated Graphene Nano-platelets xGnP

There are two grades of platelet dimensions used in the experiments within this research. The graphene nanoplatelets purchased from XG Sciences are 1 to 20 nanometre thickness with large diameters ranging between 1 to 50 microns. They are a multitude of individual platelets; this characteristic can then prevent agglomeration of groups of nano particles. Their chemical suspension can be controlled with

mechanical agitation. Successful dispersion is a function of time, energy, and the combination of used materials. Specific to the ones that are used within this project the Grade M XGnP that have an approximate thickness of 6 to 8 nanometres with a typical surface area of 120 to 150m^2/g, with 25microns in diameter size. Therefore, detailing a large diameter, but with a low aspect ratio for the M25 platelets. Whilst the C750 platelets having a high surface area where surface is affected by thickness. It is important to document that the aspect ratio in materials science is the largest dimension divided by its thickness.

Thus, the aspect ratio for the M25 grade is 3125 with the calculation below:

25000nm/8nm = 3,125nm

 And the aspect ratio for C750 grade is 666.6 with the calculation below:

2000nm/3nm = 666.6nm

The impact of aspect ratio on the platelets will determine their alignment, and how they behave in a fluid, which in this case would be electricity.

3.2.3 Synthetic Graphite

Synthetic graphite and carbon products can be put into six significant categories:

- Moulded graphite and carbon

- Vitrious, glassy carbon

- Pyrolytic graphite and carbon

- Carbon fibres

- Carbon composites and carbon-carbon

- Carbon and graphite powders and particles (Pierson, 1993).

One of the general characteristics of synthetic graphite is less anisotropy (which is preferred due to the isotropic properties that have been more desired i.e., the associations to form the more perfect graphite crystal). Vitreous carbon and fibres can be formed from polymers, carbon black can be formed from natural gas, graphite can also be formed from wood, coal, charcoal from wood and a process using animals' carcasses. The carbonisation cycle is essentially a heating cycle; organic material is turned into carbon residue via the decomposition of matter. The process temperature varies and can go up to 1300°C. The graphitisation process involves the process of coke and char and is essentially the "transformation of a turbo static-graphitic material i.e., carbon, into a well-ordered graphitic structure" (Pierson, 1993).

Here, in this process, heat can exceed 3500°C. This culminates in the structural change of coke and char into graphitic material, through a large increase in the electrical and thermal conductivities. The extent to which the graphitisation of carbon happens, is dependent on whether coke or char is configured.

3.2.4 Carbonaceous filler

Carbonaceous filler is used for its superlative rate of conductivity, to establish whether on combining with a thermoset resin, there may be a possibility of conduction which is more likely on the use of a high shear mixer that provides high revolutions (rpm) to agitate and exfoliate the nanoplatelets.

The SG powder used in this research is commercially available: CAS Number 7782-42-5, specific to graphite with a minimum 300mesh size. The graphite nanoplatelets (xGnP^{TM}) were sourced from XG Sciences USA, in two grades: M and C. Grade M has a typical surface area of 120 to 150 m^2/g, and a typical thickness of 6-8 nano

meters. The average particle diameter of M25 is 25 microns. Conversely, Grade C

particles characteristically consist of sub-micron platelets with a diameter of less than

2 microns, and a thickness typically of a few nanometres. The C750 has an average

surface area of 750 m^2/g. This combination of opposing diameter and surface area

relative to weight, is intended to study the effects of this contrast on conductivity. In

doing so, this will provide a study into the feasible capacity of the nanocomposites for

EMI.

The below table 3:1 describes the two grades of xGnP used in this thesis, and their

dimensions.

Table 3:1 Graphene nanoplatelets particle dimensions.

Product	Typical Value-Parallel to surface	Typical Value-Perpendicular to Surface	Thickness	Diameter	Surface area
Grade M25			6-8 nm	25μ	120 to 150μm²/g
Thermal Conductivity watts/metre-K	3,000	6			
Grade C750			A few nm	>2μ	750μm²/g

Table 3:2 Synthetic graphite specifications.

Product	Particle Size	Purity	Colour
Synthetic Graphite 7782-42-5	300 mesh (95% <53µm)	98.6% Carbon, 0.05% Sulphur, 0.05% Nitrogen, 0.8% ash, 0.3% Volatile, 0.3% Moisture.	Grey-black

Table 3:2 describes the synthetic graphite specifications used in this research. It must be noted that there is a rounding off error as per the specifications provided by the supplier relative to synthetic graphite specifications.

3.2.5 Bio compostable filler

Food grade powder form materials for bio-composite research are as follows:

1. Agar

2. Sodium Alginate

3. Calcium Lactate

Bio-degradable food grade powders were used in some experiments to see whether the rate of natural filler could influence the softening of epoxy resin, a thermoset resin. To test this rigorously, SG was used to research the behaviour of a naturally

degradable filler being the food grade powders, ratio on a thermoset resin, and a synthetic conductive filler.

3.3 Matrix

The Axson Epolam Resin system 2017, was commercially purchased from MB Fibre Glass mbfg.co.uk. The weight ratio of the Axson Epolam Resin, Axson Epolam Hardener is 100:30, this will be needed for manufacturing the composites. This ratio is used, as it is what the supplier recommends.

3.3.1 Epoxy Specifications

The following table 3:3 illustrates the molecular formula of chemical structure found within the matrix Axon Epolam 2017 epoxy utilised within this thesis.

Table 3:3 Molecular structures in identified epoxy resin (Pubchem,2020).

Axson Epolam 2017 Resin	Molecular Formula	Molecular Structure
Epoxide Group	C_2H_6O,	(Garnish, 1972)
Epichlorohydrin	C_3H_5ClO	
Bisphenol A (BPA)	$C_{15}H_{16}O_2$	
Two Functional epoxy Called Bisphenol A diglycidyl ether Referred to as BADGE or DGEBA, with	$C_{21}H_{24}O_4$	
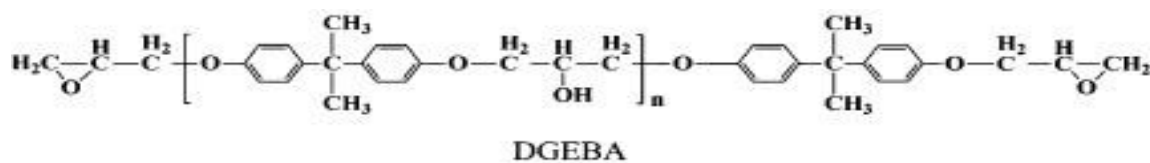
DGEBA

Figure 3-1: Molecular structure of DGEBA, (Hameed et al., 2017).

The above figure 3-1 shows molecular structure of dgeba with the terminal epoxide

groups. Epoxy resin systems are used in aerospace due to their adaptability of being

able to have higher tensile modulus with the addition of degba repetitions. They are the largest volume of thermoset resins utilised in structural aerospace composites due to their ease of processing, chemical resistance, and good mechanical properties at a material cost that is acceptable.

Below table 3:4 details information for the Axson Epolam resin used in this thesis.

Table 3:4 Axson Epolam resin DATA.

AXSON EPOLAM 2017 resin data sheet			
Name	Diglycidyl ether of Bisphenol A (BPA)	Epichlorhydrin	Trimethylolpropantriglycidyl ether
Abbreviation	BADGE/DGEBA		Not Applicable
Molecular Weight	50-100%		10-25%
	Combined Number average molecular weight. ≤700 g/mol		Not Applicable
Density at 25°C	1.17 g/cm^3 (ISO 1675:1985)		

The below table 3:5 details the main chemical ingredients found within the Epolam 2017 hardener.
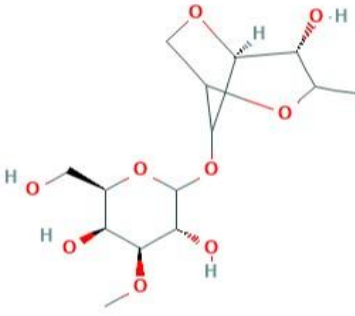
Table 3:5 Epolam 2017 Hardner DATA.
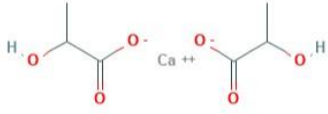
EPOLAM 2017 Hardener Data Sheet				
Chemical Ingredient Name	Polyoxyalkyleneamine	3aminomethyl-3,5,5trimethylcyclohexylamine	4-tertbutyl phenol	2,2'iminodiet hylamine
%	25-50	25-50	10-25	10-25

Density at 20°C	0.93 g/cm^3 (ISO 1675:1985)

The below table 3:6 shows the molecular structure and molecular formula of the

biodegradable food grade ingredients used in this research.

Table 3:6 Bio-compostable ingredients molecular structures (Pubchem,2020)**.**

Bio-degradable Food grade Ingredient	Molecular Formula	Molecular Structure
Agar	C14H24O9	
Na Alginate	$C_6H_9NaO_7$	

Ca Lactate	C6H10CaO6	

3.4 Methodologies of composite manufacture

A mechanical stirrer was used in all experiments to provide standard exfoliation, and mixing. Graphite has magnetic properties; thus, a magnetic stirrer is used to see whether magnetism can be used to influence the alignment of the platelets, and to research whether the use of a magnetic stirrer affects the morphology of the platelets within the composites. A sonicator was used for degassing purposes i.e., to remove air pockets from the blend mix. However, experiments that utilise further than round 1 in the manufacturing process, reintroduce gas pockets using the mechanical stirrer during round 2 and round 3. The experiments conducted were to research the impact of a longer, and leaner processing practice do preserve the platelet morphology (shape and size of the nano-platelets), using lower energy and speed in manufacturing.

3.4.1 Composite Manufacture Process 1

Round one (R1) commences with the mechanical stirrer (MechS), which is standard, with moderate to low level of rpm speed for 60 minutes. Then the second step of round 1 is the magnetic stirrer (MagS) for 90 minutes at room temperature, then the final step of round 1 is to sonicate (Son) for 45 minutes at room temperature. Round two (R2) commences with the magnetic stirrer, for 60 minutes at room temperature. Then the second step of round 2 is to sonicate for 60 minutes at room temperature.

Round three (R3) commences with the magnetic stirrer, for 90 minutes at room temperature. Then the second step of round 3 is to sonicate for 45 minutes at room temperature.

A summary of composite manufacture process 1

R1 MechS (60 m)-MagS(90m)–Son (45m)

R2- MechS(NA)-MagS(60m)- Son(60m)

R3-MechS(NA)-MagS(90m)-Son (45m)

The chemical variables in the E detailed experiments are Agar, Calcium lactate, and sodium alginate. Please note that in Experiment 8E no SG was used. For each experiment listed with a number and the letter E, describes that it is the experiments that have bio-compostable ingredients, followed by which ingredients. The number of the experiment identifies what ingredients are present in the composite.

Here is a list of the bio-compostable ingredients used that correspond to the experiment conducted.

Experiment 1E: sodium alginate only.

Experiment 2E: calcium lactate only.

Experiment 3E: agar only.

Experiment 4E: sodium alginate, and calcium lactate only.

Experiment 5E: sodium alginate, and agar only.

Experiment 6E: agar, and calcium lactate only.

Experiment 7E: sodium alginate, agar, and calcium lactate all used.

Experiment 8E: sodium alginate, agar, and calcium lactate all used but, no synthetic

graphite, and was not feasible. As the structural integrity of blend mix required the

SG filler to give structural stability.

The below table 3:7 describes the list of food grade biodegradable experiments

conducted.

Table 3:7 Bio-compostable experiments list.

	Sodium Alginate; E1	Agar; E2	Calcium Lactate; E3
Experiment 1E	X	-	-
Experiment 2E	-	-	X
Experiment 3E	-	X	-
Experiment 4E	X	-	X
Experiment 5E	X	X	-
Experiment 6E	-	X	X
Experiment 7E	X	X	X
Experiment 8E No SG	X	X	X

Where (-) none used, and (X) means ingredient used.

The materials were selected on the basis that they are transparent, with the long-term

objective to create transparent conductive graphene composites. Single layer graphene

is transparent but few layer plus graphene exhibits darker shades of grey and black.

Furthermore, these materials were selected to measure whether they influence the

epoxy matrix and the tensile strength of the combined SG and xGnP to give ductile behaviour of the composites.

3.4.2 Composite Manufacture Process 2

Round one commences with the mechanical stirrer, which is standard, with moderate to low level of rpm speed for 90 minutes. Then the second step of round 1 is the magnetic stirrer for 90 minutes with two temperature variables 34°C and 40°C, then the final step of round 1 is to sonicate for 45 minutes at either 34°C or 40°C. Composite Manufacture Process 2 only has round1. There are no other rounds. This procedure was reached to compare the effects of a shorter manufacturing process (2) consisting of Experiments 1A to 4A, and 1B to 4B, compared to the longer manufacturing process (3), consisting of experiments 1C to 4C and 1D to 4D. A summary of composite manufacture process 2:

R1 MechS (90 m)-MagS(90m) [T1] at 34°C or 40°C –Son (45m) [T2] at 34°C or 40°C

Temperature Variables: 34°C, 40°C. Chemical Variables: xGnP, and Synthetic Graphite. The below table 3:8 describes the temperature, and filler variables used in composite manufacture 2.

Table 3:8 Temperature, xGnP, and SG variable list (1).

	T1	T2	M3
Level 1	34	34	xGnP
Level 2	40	40	Synthetic Graphite

Table 3:8 describes the temperature used at the corresponding level. It also confirms the filler used at the corresponding level. An example of this is Experiment 1A with temperature 1 (T1) at Level 1 being 34°C, temperature 2 (T2) at Level 1 being 34°C using material 3 (M3) at Level 1 being xGnP. Another example is Experiment 4B with temperature 1 (T1) at Level 2 being 40°C, temperature 2 (T2) at Level 2 being 40°C using material 3 (M3) at Level 2 being SG. This description is listed below with the experiment number identifying the temperature used, and the experiment letter categorises the conductive filler used for that manufacturing process relative to its condition.

Experiment 1A: T1(34°C)-T2(34°C)-M3(xGnP)

Experiment 2A: T1(40°C) T2(34°C)-M3(xGnP)

Experiment 3A: T1(34°C) T2(40°C)-M3(xGnP)

Experiment 4A: T1(40°C) T2(40°C)-M3(xGnP)

Experiment 1B: T1(34°C)-T2(34°C)-M4(Synthetic Graphite)

Experiment 2B: T1(40°C) T2(34°C)-M4(Synthetic Graphite)

Experiment 3B: T1(34°C) T2(40°C)-M4(Synthetic Graphite)

Experiment 4B: T1(40°C) T2(40°C)-M4(Synthetic Graphite)

3.4.3 Composite Manufacture Process 3

Round one commences with the mechanical stirrer, which is standard, with moderate to low level of rpm speed for 90 minutes. Then the second step of round 1 is the magnetic stirrer for 90 minutes with two temperature variables 34°C and 40°C, then the final step of round 1 is to sonicate for 45 minutes at either 34°C or 40°C.

Round two commences with the mechanical stirrer, which is standard, with moderate to low level of rpm speed for 60 minutes. Then the second step of round 2 is the magnetic stirrer for 60 minutes with two temperature variables 34°C and 40°C, then the final step of round 2 is to sonicate for 60 minutes at either 34°C or 40°C. Round three commences with the mechanical stirrer, which is standard, with moderate to low level of rpm speed for 30 minutes. Then the second step of round 3 is the magnetic stirrer for 90 minutes with two temperature variables 34°C and 40°C, then the final step of round 3 is to sonicate for 45 minutes at either 34°C or 40°C. A summary of composite manufacture process 3:

R1 MechS (90 m)-MagS(90m) [T1] at 34°C or 40°C –Son (45m) [T2] at 34°C or 40°C

R2- MechS(60m)-MagS(60) [40°C]-Son(60)[40°C]

R3-MechS(30m)-MagS(90) [34°C]-Son (45m)[34°C]

Temperature Variables: 34°C, 40°C. Chemical Variables: xGnP, and Synthetic Graphite. The below table 3:9 describes the temperature, and filler variables used in composite manufacture 3.

Table 3:9 xGnP, and SG variable list (2).

	T1	T2	M3
Level1	34	34	xGnP
Level2	40	40	Synthetic Graphite

The above table 3:9 describes the temperature used at the corresponding level. It also confirms the filler used at the corresponding level. An example of this is Experiment 1C with temperature 1 (T1) at Level 1 being 34°C, temperature 2 (T2) at Level 1 being 34°C using material 3 (M3) at Level 1 being xGnP. Another example is Experiment 4D with temperature 1 (T1) at Level 2 being 40°C, temperature 2 (T2) at Level 2 being 40°C using material 3 (M3) at Level 2 being Synthetic Graphite.

Experiment 1C: T1(34°C)-T2(34°C)-M3(xGnP)

Experiment 2C: T1(34°C) T2(40°C)-M3(xGnP)

Experiment 3C: T1(40°C) T2(34°C)-M3(xGnP)

Experiment 4C: T1(40°C) T2(40°C)-M3(xGnP)

Experiment 1D: T1(34°C)-T2(34°C)-M4(Synthetic Graphite)

Experiment 2D: T1(34°C) T2(40°C)-M4(Synthetic Graphite)

Experiment 3D: T1(40°C) T2(34°C)-M4(Synthetic Graphite)

Experiment 4D: T1(40°C) T2(40°C)-M4(Synthetic Graphite)

Table 3:10 Materials used in this thesis.

Conductive Fillers	xGnP	Synthetic Graphite	
Bio-compostable Fillers	Agar	Calcium Lactate	Sodium Alginate
Matrix	Axon Epolam 2017 Resin/Hardener		

Composite Manufacturing Processes	1	2	3

Table 3:10 outlines all the materials used, and the manufacturing processes utilised.

3.5 Composite Fabrication Instrumentation

The mechanical stirrer (JJ-1 Precise Strength Power Mixer) has been used for this experimentation to provide gentle mechanical exfoliation. The magnetic stirrer (LKTC-B1-T) has been used in this research to intercalate the platelets and catalyse the bio-compostable ingredients. For sonication, the sonicator (LS-02D) has been used for the experiments listed above in chapter 3, to help with the removal of air pockets within the composite manufacturing processes. An unbranded pocket digital scales were used, which may have given inconsistent weight measurements.

3.6 Thermoset Wet Hand-Layup Moulding

Rubber mould is the technique undertaken to produce cavities to cure specimens, known as the toolmaking mould. The below figure 3-2 shows the stages to achieve the International Standard American Society for Testing Materials ASTM International D638 Type I using die cast and moulds.

Stage 1: Negative metal cast, tool making mould.   Stage 2: Positive rubber mould cast.
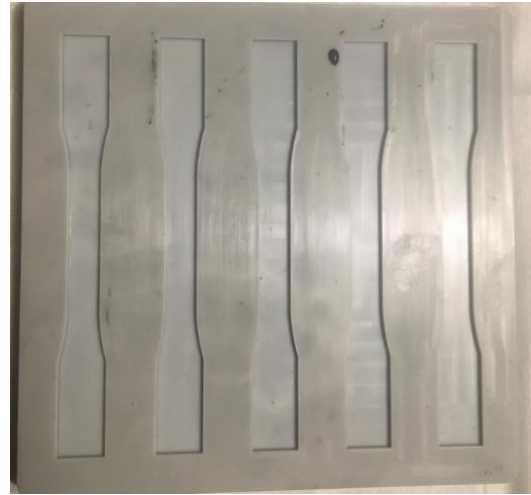
Stage 3: Layup of samples, and comparison of on the left using high temperatures, whilst on the right using SG with low temperatures.

Figure 3-2: Samples being prepared in mould, using different processing techniques of sample manufacture.

The below figure 3-3 shows the negative die cast mould used to achieve a positive rubber mould used to obtain specimens used for conductivity testing.

a)   b)
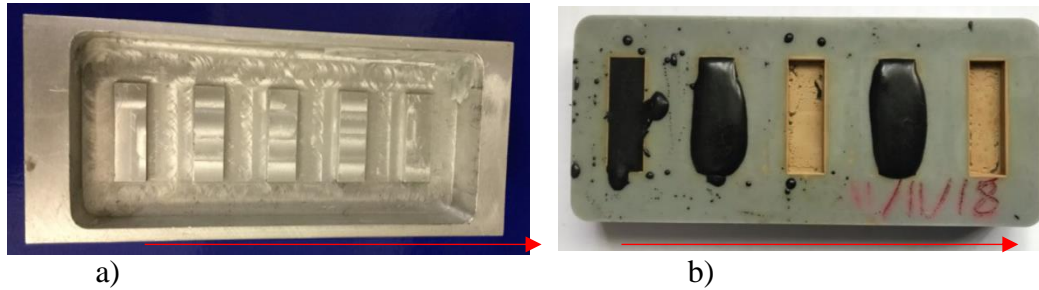
Figure 3-3: (a) Negative mould resulting in (b) Positive mould, depicting the effect given due to the handmade composites, resulting in irregular shapes of moulds.

3.6.1 Die Casting Mould processing

According to the International Standard American Society for Testing Materials ASTM D638, manufacturing of Type I composites is carried out using a steel negative cast, which is sprayed or overlayed with the Buffalo silicone lubricant. Secondly, the Buffalo silicone lubricant is shaken well before use. Thirdly, the surface to be treated is sprayed. Silicone Lubricant was used to help with the release of casted rubber mould. The shape of the ASTM standard type I used is shown in figure 3-4.

Table 3:11 Easy composites instructions to manufacture condensation rubber mould.

Ingredients	Ratio	Cast/Mould Manufacture
CS25 Condensation Cure Silicon Rubber	100:5	Measure ratio Combine ingredients Degas to the point no air pockets at surface

CS25 Condensation Cure Silicone Rubber Catalyst	5:100	Spray Silicone Lubricant onto cast Hand lay-up mould with mixture

The ratio of the silicon rubber mould followed the recommendation set out by easycomposites.com the supplier, as seen in table 3:11. The ingredients were mixed using a wooden spatula, then the next step was to degas in a degassing vacuum till no air pockets are visible. Then the negative cast was sprayed and prepared with the buffalo silicone spray lubricant, and finally layup of the negative cast with the silicon rubber blend mix was prepared.

The below table 3:12 describes the ASTM D638 Standard Test Method for Tensile Properties of Plastics specifications.

3.6.2 Specifications of ASTM D638 Type I specimens:

Table 3:12 Specifications of ASTM D638 Type I specimens.

Dimensions	Type I
W-Width of narrow section	13mm
L-Length of narrow section	57mm
WO-Width overall	19mm
LO-Length overall	165mm
Gage length	50mm
D-Distance between grips	115mm
R-Radius of fillet	76mm
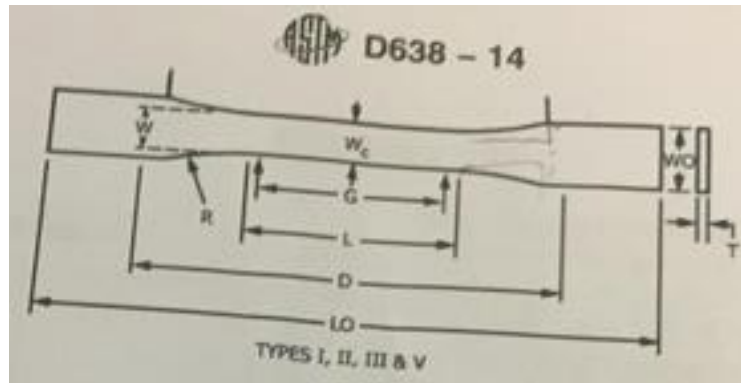
Figure 3-4: The ASTM D638 standard Types I, II, II & V.

3.6.3 Conductivity Specimens

Below (figure 3-5) is the plan for the die cast moulds specifications for the conductivity specimens. A negative die cast mould is used from which a positive rubber mould can be made.
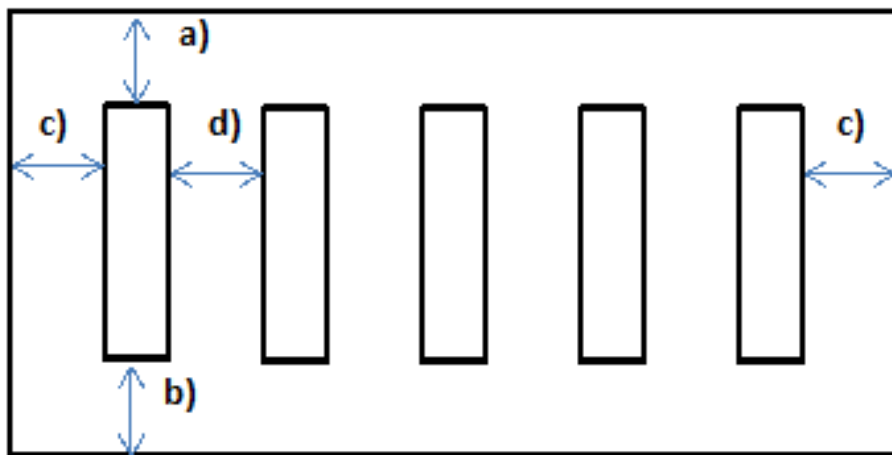

Figure 3-5: The negative die cast mould blueprint of conductivity specimens, with corresponding letters to outline the spatial mould measurements outlined below.

The Spatial Mould measurements are:

a) 10mm top spacing

b) 10mm botttom spacing

c) 10mm Lateral ending

d) 15mm spacing between negatives

The width of each specimen mould is designed to be 1cm, with 3cm for length, and 3mm for thickness, with the depth of mould is required to be a minimum 15mm thicker than the negatives.

3.7 Composite characterisation methods

The characterisation techniques that are utilised in this research are: tensile testing systems, morphological studies utilising laser and light microscopy, heat-analysis softening techniques, and finally the measurement of conductance in ohmic values. Shielding Effectiveness will not be measured as this requires composites in metres in length and width. Resources to manufacture this size of composites is limited.

3.7.1 Tensile

Instron 3344 tensile testing machine was used to find if there any the influences on composite manufacture, and the ingredients used on the properties and mechanical behaviours of the test specimens. Tensile testing was performed on cured tensile specimens using a crosshead speed of 5cm/minute, as identified by Sharma et al (2016). The standard that was followed for this type of testing corresponds to ASTM D638 Type I. The total number of tensile specimens produced for each condition is 10. Then to take into account failed testing, the average number of specimens tested

for each condition is approximately 5, though some were over 6. However, the Instron 3344 did take some unreliable readings. These were not used. There are 8 conditions for each composite manufacture, so:

$$8 \times 3 \ (types \ of \ composite \ manufacture \ processes) = 24 \ conditions$$

However, experiment 8E experienced crash out so no specimens were produced. So:

$$23 \times 10 \ (tensile \ specimens) = 230 \ (including \ failed \ tests).$$

Accounting for the non−failed tests is: $23 \times 6 = \approx 138 \ tested \ tensile \ spcimens$.

3.7.2 Morphological, topological, crystalline

The Quanta 200 Scanning Electron Microscopy (SEM) was used to study the morphologies of the specimens at an accelerating voltage of 10kV to a maximum of 30kV, with varying magnifications. Tagarno FHD Trend Microscopy was used for a view of nanoplatelets under day light conditions compared to electron lighting, to review behaviours such as reflectance that are not visible with Quanta 200.

3.7.3 Electrical Resistivity Measurements

The electrical resistance measurements of xGnP, and SG nanocomposites were preformed using 600V AC/DC Digital Multi metre, manufactured by DURATOOL, and measuring up to 66 MΩ. In addition, for a calibrated and accurate reading, specimens were also measured using the Keithley 34450A multimetre, measuring up to 100MΩ. Essentially, the only two resistance measurement instruments used were calibrated using the Vishay Z Foil Resistor with an electrical resistance of 100Ω (0.005 %).

Chapter 4 - Results and Discussion

4.1 Visual Inspection of Mixtures

This section provides evidence of clustering in the Composite manufacture process 3, in natural xGnP (Experiments 1C, 2C, 3C, and 4C) with some description of temperatures used. These images are not ideally taken, they are hindered with reflections. Cross section view under SEM would be investigated in the future; however, this was during manufacturing. So, transferring the blend mix from the processing laboratory to the Quanta 200 laboratory would have been difficult.

a)   b)   c)
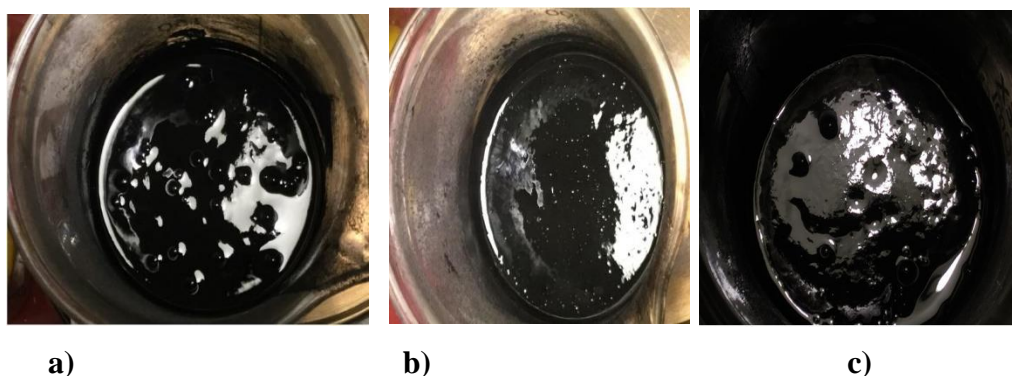
Figure 4- 1: (a)Experiment 1C using xGnP during blend mix processing, (b) Experiment 2C, xGnP during blend mix processing, and (c) Experiment 3C, xGnP during blend mix processing (tar-like).

Figure 4-1: (a) Experiment 1C using xGnP with temperature 34°C in T1and T2. The natural xGnP is forming agglomerates and cluttering during mechanical stirrer. This image shows that the blend mix requires further processing and mixing as the mix is still heavy viscosity.

Figure 4-1: (b) Experiment 2C using xGnP with temperature at T1 34°C, and at T2 40°C. Post-sonication the clustering had become more refined, with smaller sized clustering. This is evidence of better particle dispersion, as the blend mix is light and fluid. However, heavier platelets sediment to the base of the beaker.

Figure 4-1: (c) Experiment 3C using xGnP with temperature at T1 40°C and T2 34°C. Nano-mix behaving tar-like, heavy globules of highly viscose blend mix. Emitting tar-like aroma. The temperature commencing at 40°C for round 1 at the magnetic stirrer, shows that introducing heat early on in the manufacturing processing without tempering heat progressively can result in crash out. However, T2 is at 34°C so heat is managed and not over exposed or processed.

a)   b)   c)
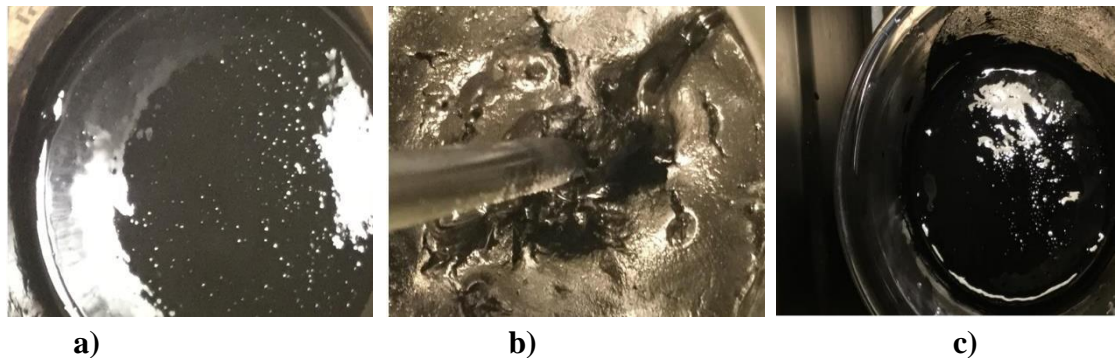
Figure 4-2: (a) Experiment 3C, xGnP during blend mix processing (miniature bubbles), (b) Experiment 4C, xGnP during blend mix processing (top layer viscous), (c) Experiment 4C, xGnP during blend mix processing (sonification effect).

Figure 4-2: (a) Experiment 3C, xGnP with temperature at T1 40°C and T2 34°C. Approximately 40 minutes later during sonication, blend had become a lot more refined, and the consistency was more fluid. As it can be seen that the air pockets within the blend mix had reduced in size, shape and dispersion.

Figure 4-2: (b) Experiment 4C, xGnP with temperature at T1 40°C T2 40°C. Blend mix had stiffened after a full processing of round 1. This is at the initial application mechanical stirrer into the blend mix that had somewhat undergone sedimentation, where heavier particulates subside to the base and lighter one's float to the top. Both T1 and T2 are at 40°C, with xGnP having high thermal conductance, and the epoxy

matrix having a much lower heat resistance. This provided the situation of the epoxy being projected to heats at the higher levels of its heat tolerance, whilst the xGnP not near its heat tolerances. This situation of polar opposites within the thermal scale has caused the blend mix to emit a very potent tar-like smell, and blend mix behaviour.

Figure 4-2: (c) Experiment 4C, xGnP with temperature at T1 40°C T2 40°C. This post-sonication of the last process of experiment 4C. Blend mix has blended better than at the beginning of processing. However, clustering is still prevalent. Heat, and processing had caused the blend mix to become more heavier with a higher viscosity, yet the blend mix is better dispersed than at round 1 of Composite Manufacture 3.

Here is some evidence of more smooth mixture during composite manufacture 3, in synthetic graphite including (Experiments 1D, 2D, 3D, and 4D).

a)   b)   c)

Figure 4-3: (a) Experiment 1D, SG during blend mix processing (fluid), (b) Experiment 1D, SG during blend mix processing (air pockets), (c) Experiment 1D, SG during blend mix processing (after final round).

Figure 4-3: (a) Experiment 1D, SG with temperature at T1 34° C T2 34° C. Here it is visible to see that using a form of synthetic graphite the front layer of blend mix shows a good dispersion or lacking globule platelets, and reduced clustering of

platelets. The blend mix is very fluid, and the epoxy has not been influenced by heat or the thermal conductance of synthetic graphite.

Figure 4-3: (b) Experiment 1D, SG with temperature at T1 34°C T2 34°C. Later through processing of round 2 during magnetic stirring, bubbling began to form, thus influencing clustering to reform. Here, there is a large content of air pockets within the blend mix during sonication, which is the process of air pocket removal. The air pockets get smaller over the time of degassing using sonication, and the distance between them gets scarcer. So, the density of the air pockets becomes less and less with more subjection of the blend mix to sonication. However, within all experiments the lighter platelets float to the top of the blend mix, and the heavier bulkier agglomerations of platelets subside to the base of the beaker.

Figure 4-3: (c) Experiment 1D, SG with temperature at T1 34°C T2 34°C. This is during the final process of round 3, where the blend mix does not show bubbling or clustering of synthetic nanoparticles. When using lower temperatures, the blend mix is not as catalysed or challenged, as the platelets would have been using higher temperatures. Using higher temperatures causes higher energy mixing, that leads to added bubbling. There is no evidence of heat caused bubbling during Experiment 1D. However, during experiment 4C and 4D where the temperature for T1 and T2 is 40°C, there is evidence of bubbling forming, which causes the blend mix to have a foam like behaviour.

a)   b)   c)

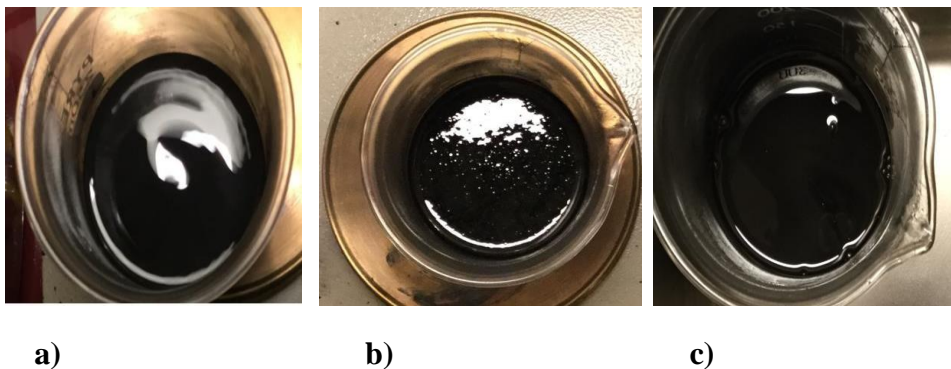**Figure 4-4: (a) Experiment 2D, SG during blend mix processing (round 2), (b) Experiment 2D, SG during blend mix processing (round 3 electric stirrer), (c) Experiment 2D, SG during blend mix processing (round 3 sonification).**

Figure 4-4: (a) Experiment 2D, SG with temperature at T1 34°C T2 40°C. Here during magnetic stirring of round 2, the blend mix is fluid, with no visible clustering.

Figure 4-4: (b) Experiment 2D, SG with temperature at T1 34°C T2 40°C. At the commencing of round 3, showing SG grouping, clustering but no stiff top of blend mix. However, foam behaviour of the blend mix is caused by heat bubbles and agglomeration of platelets.

Figure 4-4: (c) Experiment 2D, SG with temperature at T1 34°C T2 40°C. During sonication of round 3, blend mix had settled and sedimented. There were less obvious air bubbles in the blend mix emitting a tar-like smell, and the blend mix behaviour showed a lower viscosity compared to Experiment 4C.
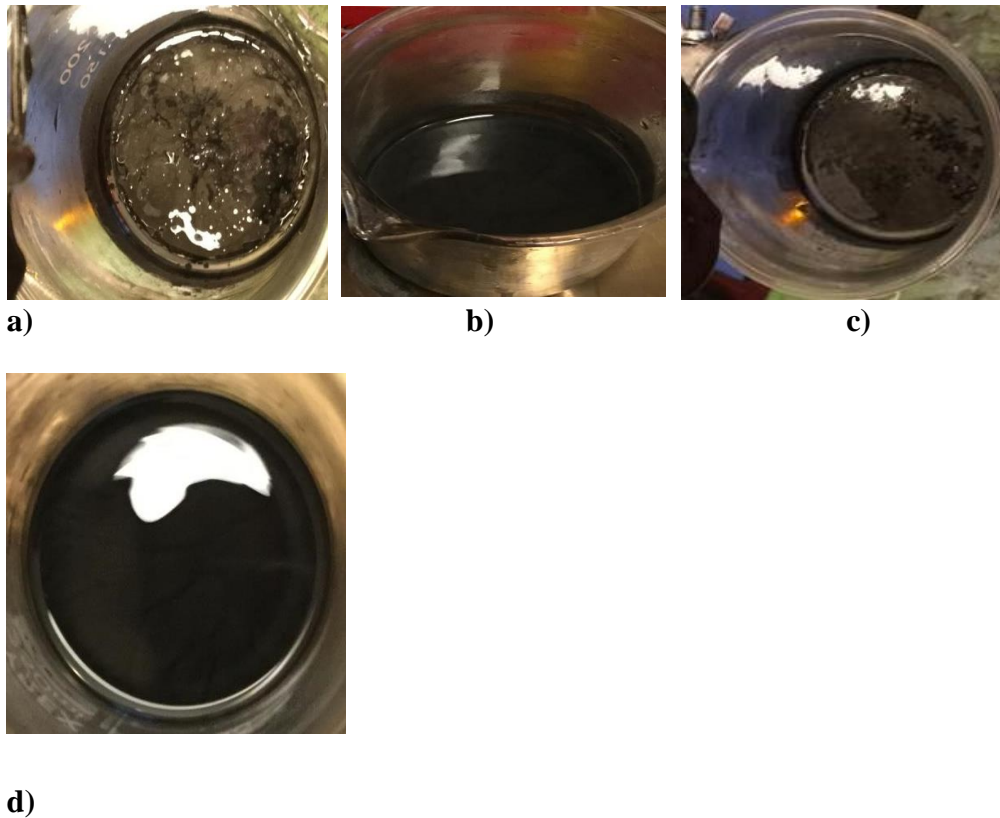
a)

b)

c)

d)

Figure 4-5: (a) Experiment 3D, SG during blend mix processing (round 2 electric stirrer), (b) Experiment 3D, SG post full processing, (c) Experiment 4D, SG during blend mix processing (post round 1), and (d) Experiment 4D, SG post full processing.

Figure 4-5: (a) Experiment 3D, SG with temperature at T1 40°C T2 34°C. At the initial commencing of round 2. It can be seen there are smaller clusters than in the same experiment using xGnP, which is a general behaviour of SG (Experiments 1D, 2D, 3D, 4D, and 1B, 2B, 3B, 4B). However, the contrast of the blend mix, platelet behaviour can be better observed with a longer leaner manufacturing process as is the comparison of Composite Manufacture 2 and 3. In this Figure 4-5: (a) the mechanical stirrer will thoroughly re-mix, allowing the SG nanoplatelets to be more influenced by magnetic mixing, and then by sonication, the releasing of air bubbles.

Figure 4-5: (b) Experiment 3D, SG with the temperature at T1 40°C T2 34°C. This is post-mixing, as you can see the blend mix is fluid, and with no obvious bubbles. This in contrary, of the same experiment but using a different carbonaceous filler; xGnP experiment 3C.

Figure 4-5: (c) Experiment 4D, SG with temperature at T1 40°C T2 40°C. Post round 1, you can see much smaller groupings of clustering than in experiment 4C, with the same conditions but different carbonaceous filler; xGnP experiment 4C. This is to do with the property of the synthetic graphite having been synthetically manufactured.

Figure 4-5: (d) Experiment 4D, SG with temperature at T1 40°C T2 40°C. Post full processing at round 3. The blend mix is fluid, though exhibited is some level of sedimentation, but not to the extent of experiment 4C. Thus, utilising a synthetic carbonaceous filler, give a different result as compared to natural graphite, graphene filler. When using synthetic graphite the blend mix bears a lighter viscosity, with less agglomerations of the blend mix.

4.2 Tensile Data Analysis

A 2kN load cell with 2kN clamp grips were used in the tensile testing of dog-bone shaped specimens in the D638 specification. The software to generate the data was Bluehill Universal.

This next section focuses on the bio-compostable ingredient composites.
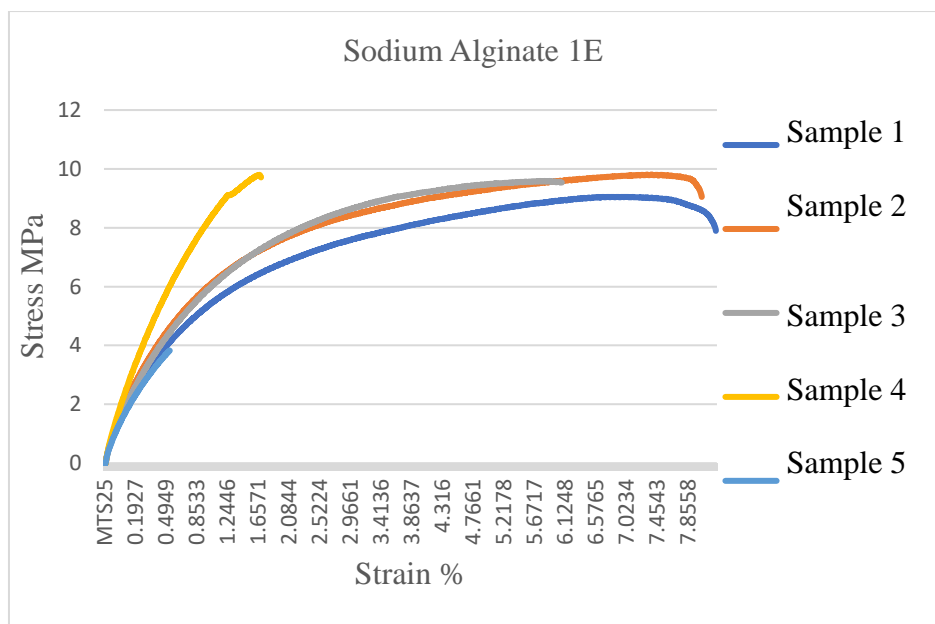
Figure 4-6: Tensile testing for experiment 1E using only Sodium alginate.

Here in Figure 4-6: the material necked at Ultimate Tensile Strength (UTS), which is at the highest load. The specimens have failed plastically, which is why the line in the graph has turned downwards, as the material gets thinner and the load drops, as there is less resistance to load in sample 1 and 2. This shows a ductile break. The light orange line being sample 4 shows that it is a stronger specimen. However, this could be an error with the cross-sectional measurements prior to testing. The more ductile the specimen, means the specimen would stretch for longer, whilst brittle specimens

break with no change to the over length as shown in ductile specimens. Out of all

experiments E, the sodium alginate only experiment 1E exhibits the most ductile

behaviour, thus the greatest stretch of specimens for longer. Sample 5 is in

contradiction to samples 1 and 2, this maybe an error when setting the specimen to be

tested.
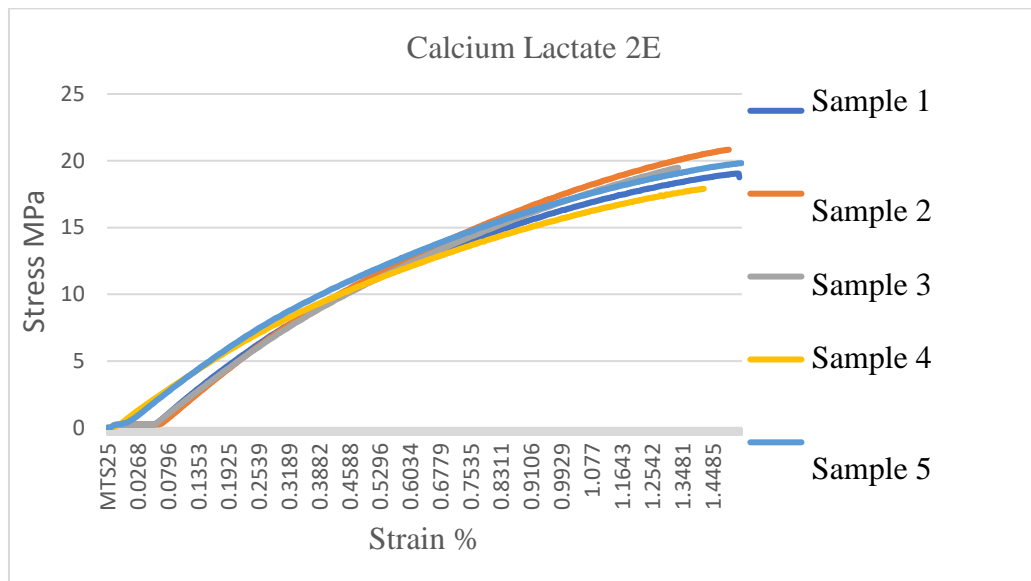
Figure 4-7: Tensile behaviour of Experiment 2E, using only Calcium Lactate.

This Figure 4-7: shows the change in the overall length is at least 5x smaller than that

of figure 4-6, which means a less ductile composite batch. It can be seen here that

because the line graph turns downwards, which as the specimens get thinner and the

load drops due to lowered resistance to load. Exhibiting a ductile break, as seen in

Figure 4-6, although at a much smaller %. This means that the specimens have failed

plastically.
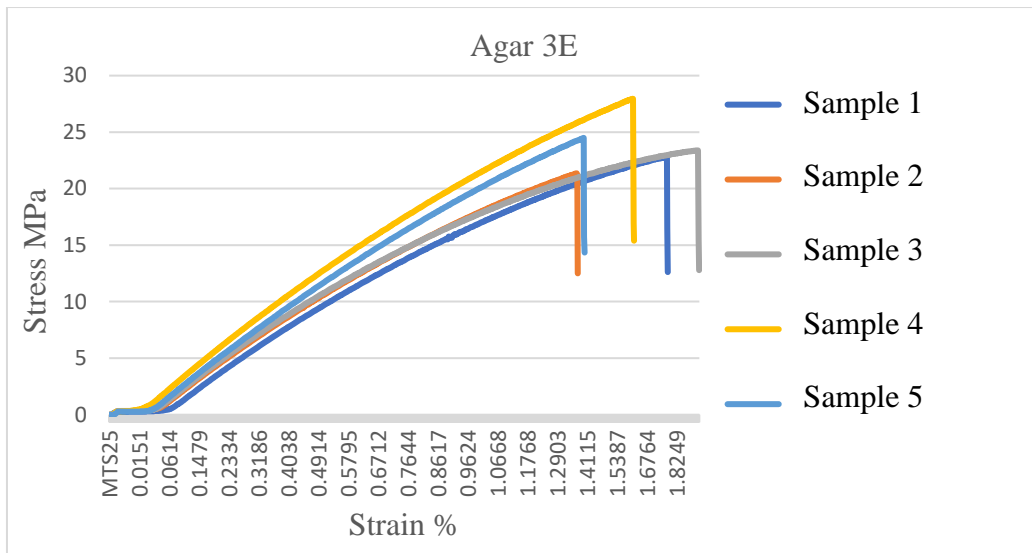
Figure 4-8: Tensile behaviour of Agar only bio-composites; experiment 3E.

These specimens of Figure 4-8: are the second most ductile of experiments list E, which are the bio-compostable ingredient composites. There is some curvature of line, which means that the samples have failed plastically, and that there is a lesser resistance to load to figure 4-7 but greater resistance to 4-6. Thus, agar provides slightly more ductility to the specimens than that of calcium lactate, whilst sodium alginate provides greatest ductility when used alone.
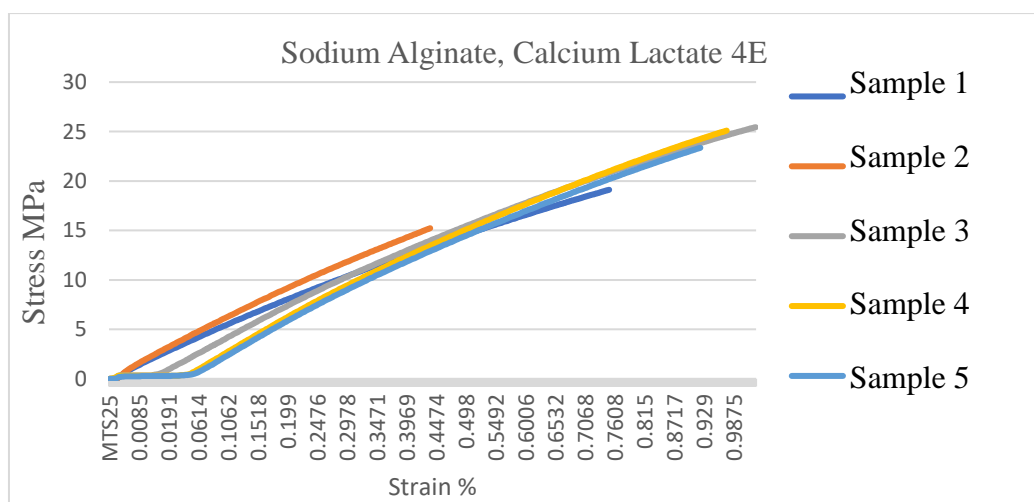
Figure 4-9: Tensile test results for experiment 4E using sodium alginate, and calcium lactate.

Here in figure 4-9: showing samples using sodium alginate, and calcium lactate take a lot of stress to break, and do not change in length from the original length as compared to other samples such as experiment 1B (14.2%). However, they change from the original length over four times than that of experiment 4D (2.4%). The strain percentage is near to 1%. The reading for sample 4 and 5 shows there were some issues with initial commencing of testing.
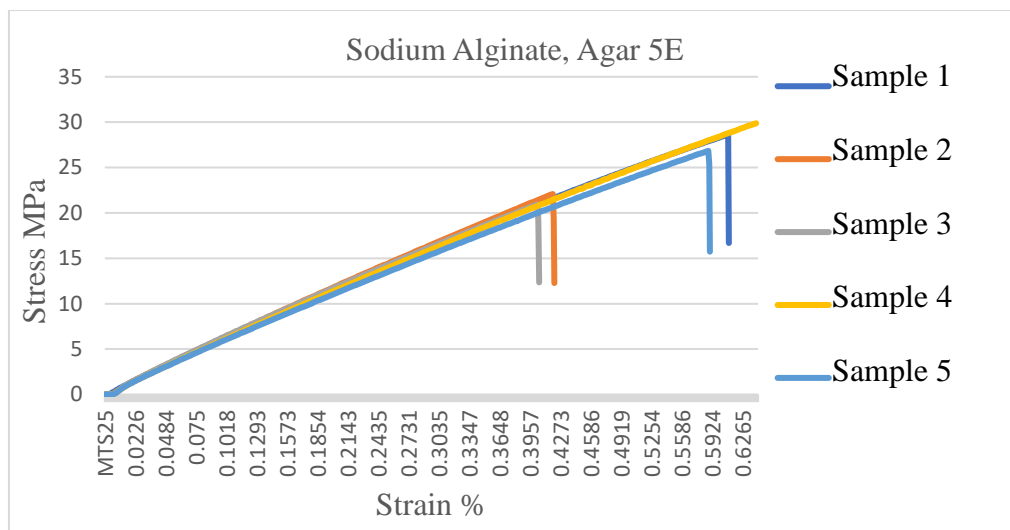
Figure 4-10: Tensile behaviour of Experiment 5E using Sodium alginate and Agar.

Here in Figure 4-10: this batch shows the strongest resistance to load of experiment list E, which means faster breaking of samples. Sample 1, and 4 show greater strength, with biggest change in the overall length of experiment 5E. This means that sample 1 and 4 have both the greatest ductility, and strength of experiment 5E. However, experiment 5E exhibits least strain of the bio-compostable composites.
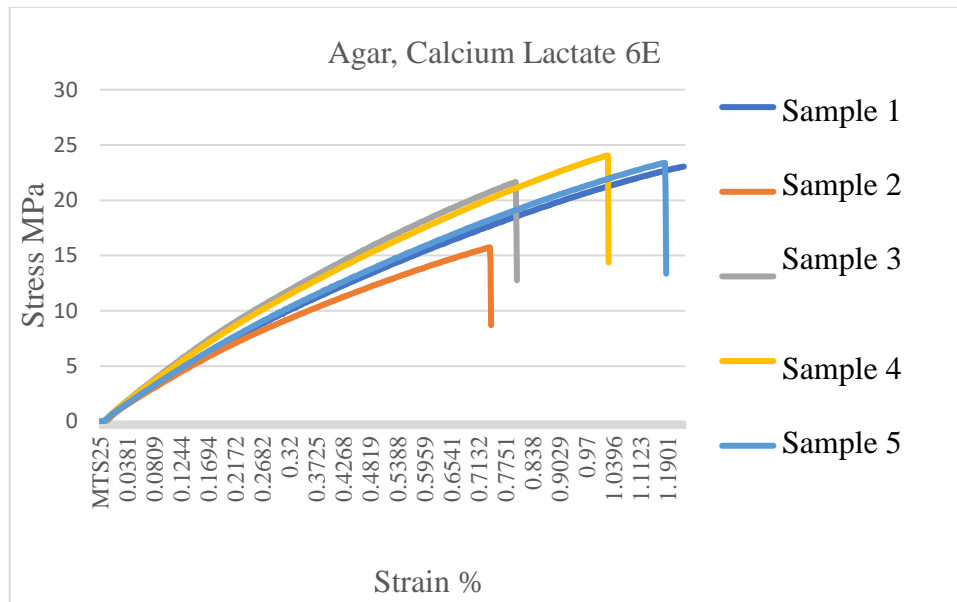
Figure 4-11: Tensile behaviour of Experiment 6E using Agar and Calcium Lactate bio-compostable ingredients only.

As shown in figure 4-11: the line graphs are not stacked on each other, which means that there are variations of platelet agglomerations, and that the dispersion of the platelets are not as uniformly combined within the blend mix as evident in the other tensile testing behaviour of experiments E. Furthermore, with the exception of experiment 3E, where there is a greater variation of data, and experiment 7E. Here in figure 4-11: shows greater strain than that of experiment 6E, this means that combining calcium lactate with agar provides greater ductility than the combination of sodium alginate with agar. This is in contradiction with experiment 1E, where the use of sodium alginate only provides greatest ductility of experiments E.
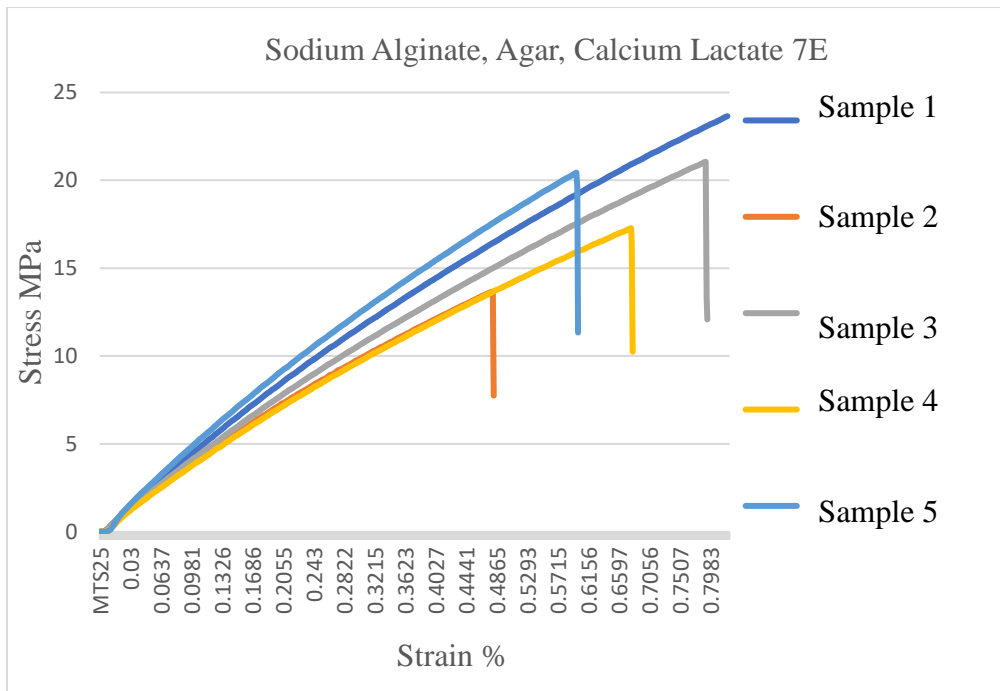
Figure 4-12: Tensile behaviour of Sodium Alginate, Agar, and Calcium Lactate bio-compostable composites.

In this figure 4-12: there is a variation of results, with the least strain 0.4877% leading to a maximum result of 0.797%. This experiment 7E shows the least strength, with the lowest ductility except for experiment 5E. The results in figure 4-12: show when combining all the bio-compostable ingredients, gives a weaker and brittle batch. Where the line graph drops, this is the break point of the samples i.e., sample 5 and 2.

This next section focuses on the composites made using Composite Manufacture 2.
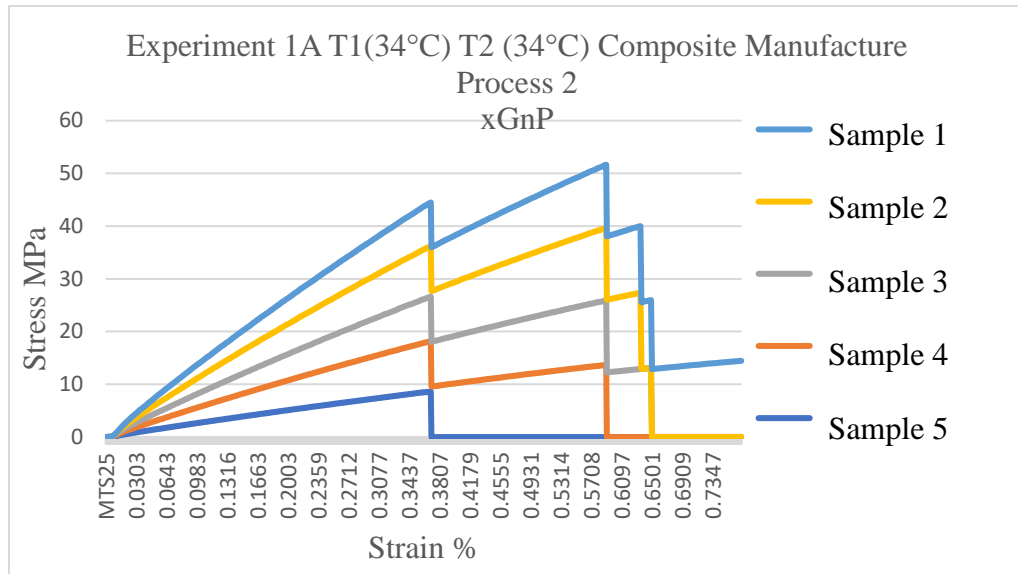
Figure 4-13: Tensile test results for Experiment 1A.

In figure 4-13: displays the slipping of sample from either grip, even when emery paper was used to provide friction to hold the samples stable. The samples utilising heat even at 34 or 40 degrees in T1 or T2 show more slippage as compared to experiments E; bio-compostable composites. This means that the heat-treated experiments have a smoother plane, compared to the E experiments, where the un-melted or un-combined bio-compostable ingredients provide friction and better grip stability. Both sample 1 and 5 specimens have not undergone failure, in-fact the specimens had slipped. The specimens are of the same batch, yet the modulus is different, exhibiting different slope values. The same batch of material should show the same slope stacked up on top of each other. However, due to the use of intercalation as a form of mixing, the tensile data results show that the platelets are not uniformly dispersed. It can be said that platelets are dispersed throughout the batch within individual groupings throughout the blend mix. This is shown up on lay-up of blend mix into the moulds, where the blend mix has a variation of consistency.

Though, this is more prevalent with synthetic graphite experiments using the highest temperature at 40°C for both T1 and T2. This results in a variation of platelet dispersion within the same batch in both xGnP, and SG heat treated composites. The platelets are in essence individually floating throughout the blend mix, in agglomerations, which is then exhibited in the tensile data.
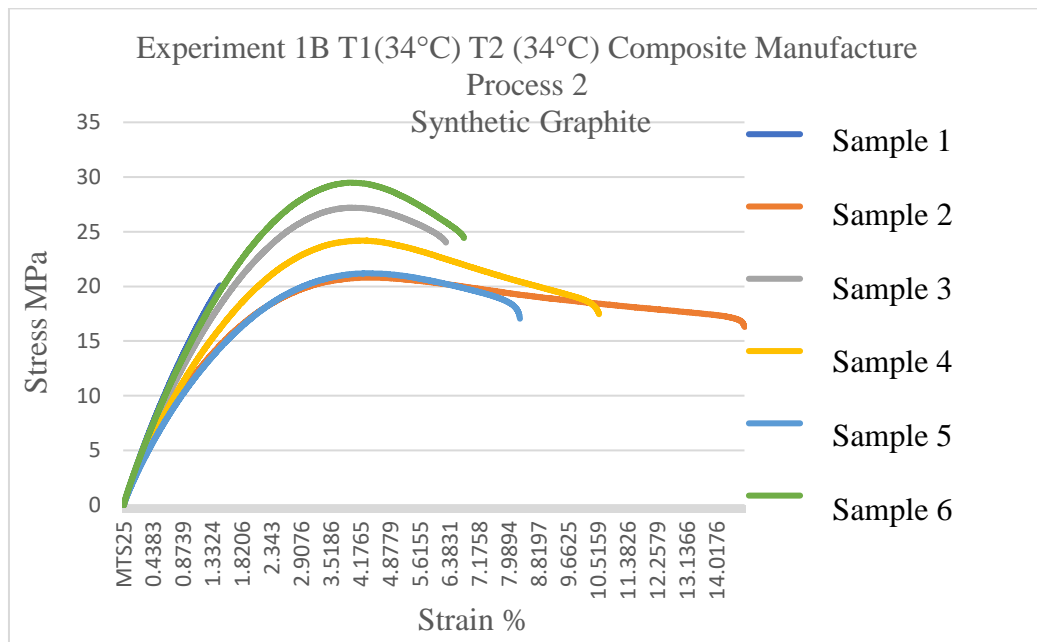
Figure 4-14: Tensile test results for Experiment 1B.

Here in figure 4-14: sample 5 reaches a near 30MPa, whilst sample 2 exceeds 14% strain from the original length of the specimen. These results all exceed 20 MPa but varied in strain percentages. This shows that using the temperature of 34°C for T1 and T2 for an experiment which only utilises one round as compared composite manufacture 3 which has 3 rounds, results in samples that are moderately strong, and bear higher levels of strain percentage. Figure 4-14: shows that the material necked at Ultimate Tensile Strength (UTS), which is at the highest load, which is similar to figure 4- 6 experiment 1E. The specimens have evidently failed plastically, which is why the line in the graph has turned downwards, as the material gets thinner and the

load drops, as there is less resistance to load in sample 2 and 4. Exhibiting a ductile break. As a matter of fact, experiment 1B shows greatest ductility of all experiments conducted. Sample 1 could be an error with the cross-sectional measurements taken prior to testing, as it contradicts other samples within the same batch.
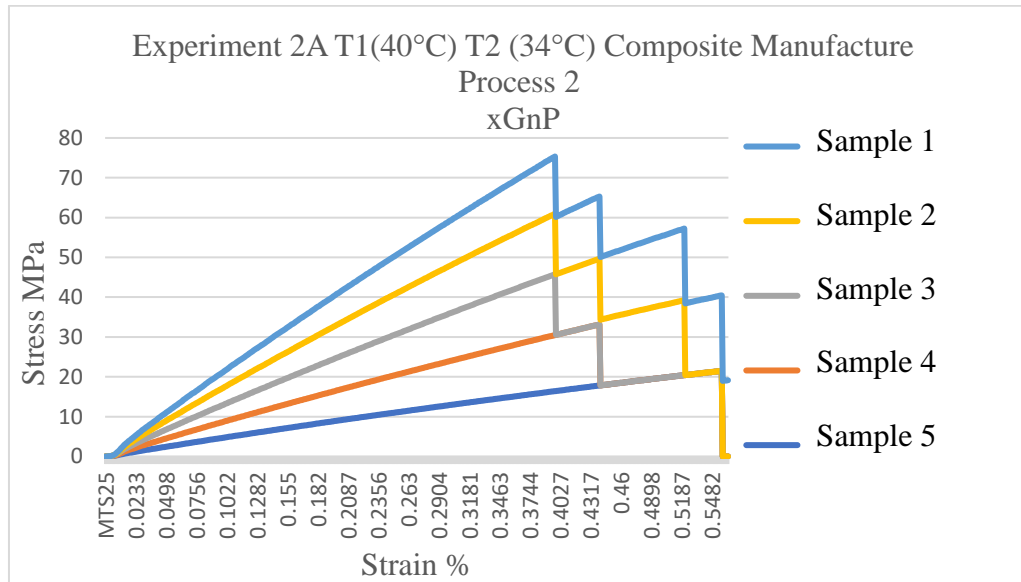
Figure 4-15: Tensile test results for Experiment 2A.

In figure 4-15: shows that the slipping of the samples from either grip, even when emery paper was used to provide friction to hold the samples put. The samples utilising heat in T1 at 40°C and T2 at 34°C show less slippage as compared to experiment 1A figure 4-13. This may mean that higher subjection to heat give a less smooth plane. Both sample 1 and 2 specimens have not undergone failure, in-fact the specimens had slipped. Again, the specimens are of the same batch, yet the modulus is different, exhibiting different slope values, which theoretically the same batch of material should show the same slope stacked up on top of each other. As discussed in figure 4-13: the process of using intercalation to combine the blend mix has evidently produced a variation of results within the same batch.
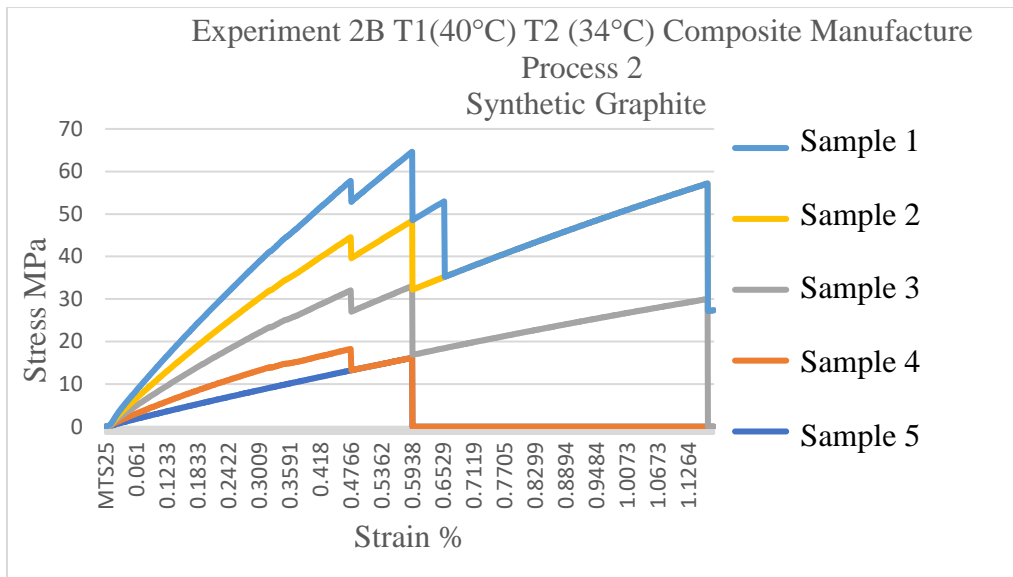
Figure 4-16: Tensile test results for Experiment 2B.

Here in figure 4-16: reiterates the observation that using intercalation as a means of dispersion of blend mix produces a smooth exterior to the composites, which cause slippage of specimens. However, the smoothness of the composite's exterior may mean that the intercalation procedure produces some form of alignment of platelets, which does not necessarily mean an unstable composites, but a smoother exterior.
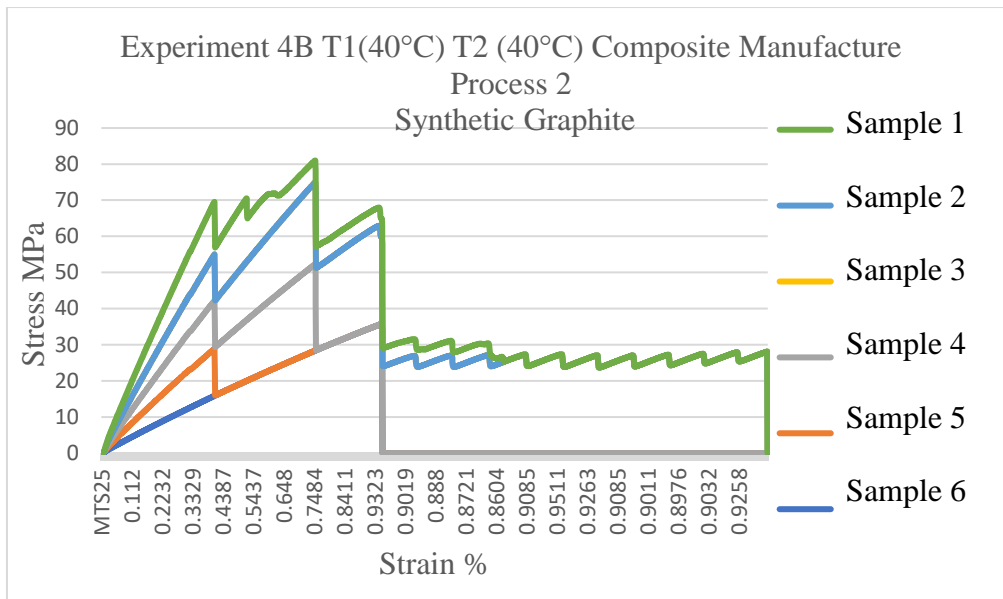
Figure 4-17: Tensile test results for Experiment 4B.

In figure 4-17: shows the tensile behaviour of experiment 4B, which consists of only round 1, yet the temperatures used in processing of T1 is 40°C and T2 is also 40°C. Comparing this to experiment 4C figure 4-18, there is more repeated slippage in figure 4-17. Again, this maybe to do with the blend mix to only have been subjected to one round, which may mean that the blend mix is not as well combined as experiment 4C figure 4-18. Both experiment 4B and 4C are subjected to 40°C in T1 and T2.

This next section focuses on the composites made using Composite Manufacture 3.
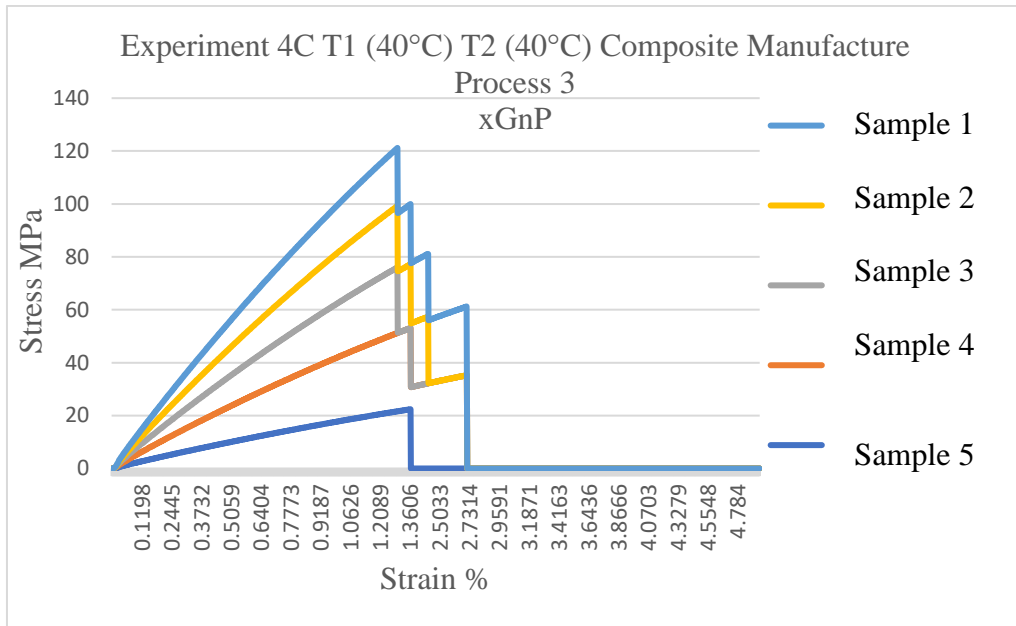
Figure 4-18: Tensile test results for Experiment 4C.

Here in figure 4-18: even with the use of emery paper, and a total of 3 rounds at 40°C in both T1 and T2, shows slipping tendency of sample from both the top and bottom grip. Though, the slippage behaviour is less than that of experiment 1A figure 4-13 and experiment 4B figure 4-17. In the case of figure 4-13: the temperature used in T1 and T2 is both at 34°C, yet in 4B is at 40° in both T1 and T2. This may be contrasting, as slippage persists at low or higher temperatures, despite the number of rounds used during processing, yet higher strain values are exhibited in figure 4-13 and figure 4-17, where in both cases only one round of processing was used.
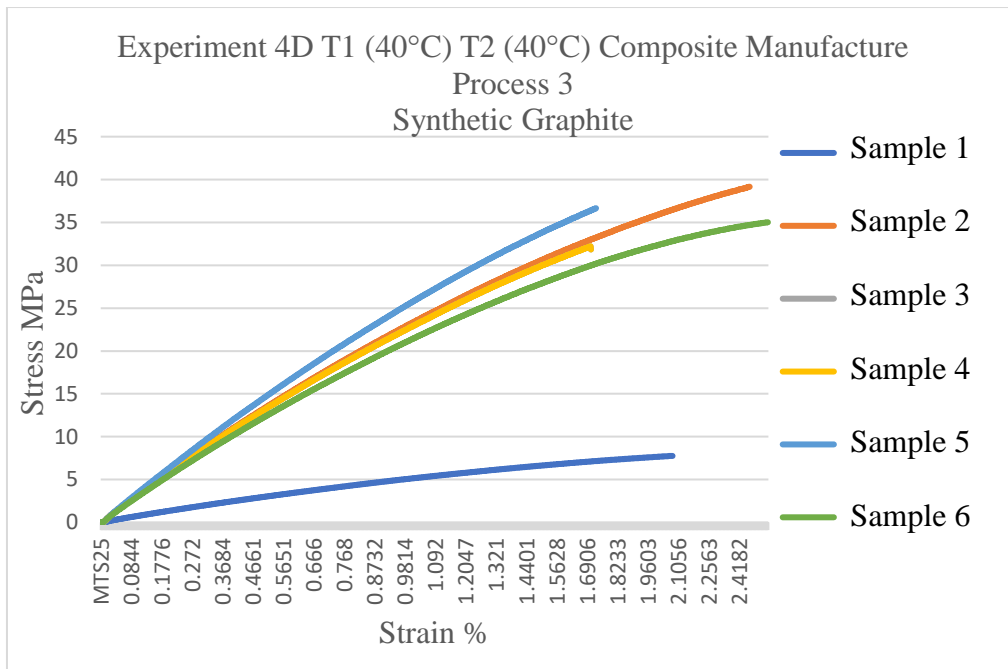
Figure 4-19: Tensile test results for Experiment 4D.

In figure 4-19: the majority of test results exceed 30MPa, whilst they all do not reach 2.5% strain. Though, they do exhibit no slippage of samples, they however, are not stacked above each other on the tensile data line graphs. As stated before, the material from the same batch should have the same slope values, which in this figure 4-19 they do not. These samples show more strength compared to other experiments such as 2A,2B and 4B. Comparing experiment 4D, to 4B and 4C which all use the higher temperature of 40°C in both T1 and T2, 4D does not show any slippage of sample from either grip. The difference in processing is that 4D, and 4C have a total of three rounds, and utilise the Manufacturing Process 3, whilst experiment 4B only uses round 1 of processing composing of Manufacturing Process 2.

4.3 Conductivity Results

To measure electrical resistance of xGnP, and SG nanocomposites two multi-metres were used: 600V AC/DC, and Keithley 34450A.
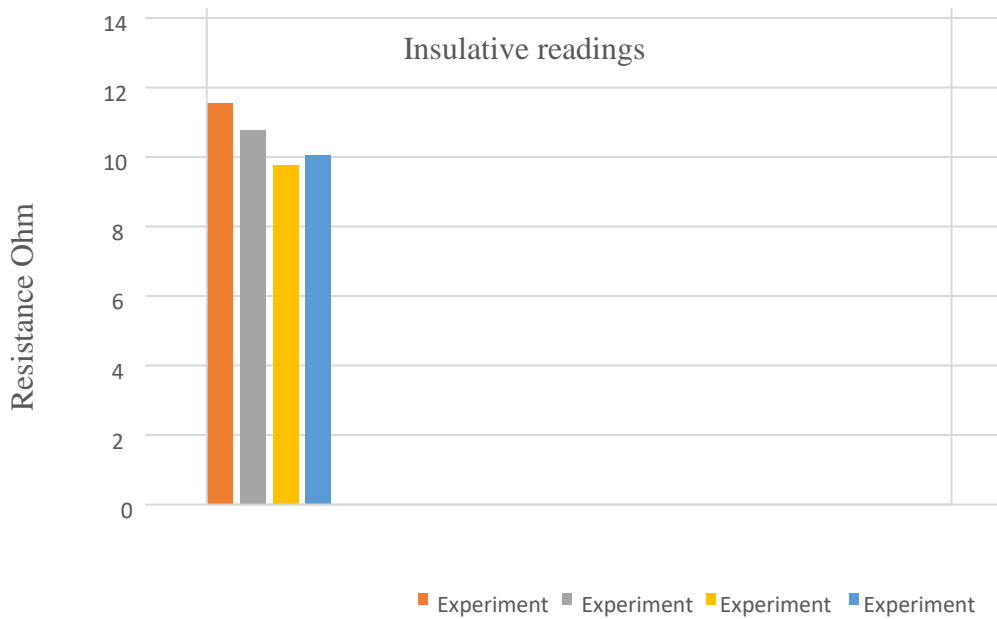
Figure 4-20: Electrical resistivity test.

In figure 4-20: overall, the manufactured samples showed no conduction, however
with some gentle polishing they became very conductive. The SG samples showed
higher resistivity. The gentle polishing removed some of the outer layer of the
insulative epoxy and gave exposure to the conductive graphite. Many repeat
resistance measurements were made, and the data spread was overwhelming of high
resistance. In some cases, no measurements were able to be made due to the insulative
nature of the epoxy, and the manufacturing processes. Comparing these results with
other shielding material, makes them very highly resistant to conduction, whilst other
shielding materials tend to have a much higher level of conduction values.

Figure 4-21: Placement of resistance measurement terminals using the 600V AC/DC multi-meter.

Using the electron tunnelling theory, electricity finds the easiest and quickest route for it to travel. It was necessary to measure the specimens in both the top and bottom plane to see whether any conduction values are recorded, as seen in figure 4-21. This was not found to be case, where specimens were all thoroughly resistive.

4.4 Visual Inspection of samples based on reflectance

The Quanta 200 Scanning Electron Microscopy (SEM) is used here to study the morphological nature of the specimens at an accelerating voltage of 10kV to a maximum of 30kV, with varying magnifications.
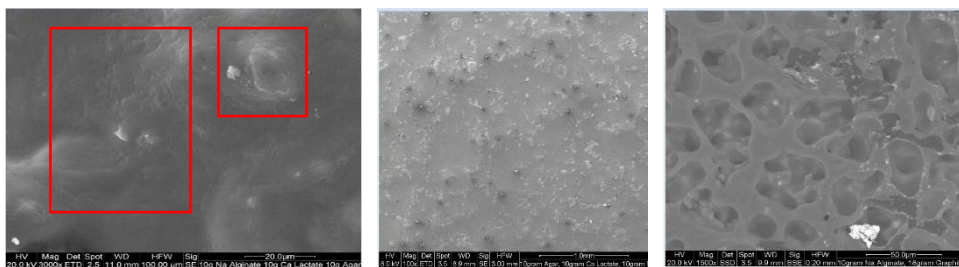
a)   b)   c)

Figure 4-22: (a) The morphology of Experiment 7E SEM (20.0μm) of sodium alginate, calcium lactate and agar, (b) the morphology of Experiment 7E SEM (1.0mm) with Agar and Calcium lactate, (c) the morphology of Experiment 1E (50.0μm) of sodium alginate.

In figure 4-22: (a) a low magnification, which displays the layers SG platelets subsided in the a-b plane. The a-b plane is the horizontal plane to the c axis. The a-b plane is shown in figure 4-23, as seen below. It is visible to see with the SEM that agglomerations of synthetic graphite layers are prevalent with approximately 5µm sized cross sections of the conductive filler, and large sized food grade ingredients that display a different texture to the synthetic graphite.

In figure 4-22: (b) this image shows the bio-compostable food grade ingredients to not melt or be influenced during processing especially the Ca Lactate, however the agar does dissolve due to the influence of mixing with the epoxy. The surface area is evident to not be smooth. This is visible without the use of microscopy. All E experiments are discussed in Chapter 3, including the methodology of constructing all experiments. Big rough, ragged edges of sodium alginate, and calcium lactate are visible throughout the specimen. This is an indication of insufficient mixing of substituents.

In figure 4-22: (c) the use of sodium alginate suggests some form of fermentation bubbling behaviour between the epoxy, SG, and Na Alginate. This can be seen at the surface of the composite when placed under the SEM. This could be due to repulsed reactions between the ingredients that causes a chemical break of bonding. It may be said that the use of sodium alginate here seems to display gum-like stretching of the blend mix. In-addition, the large particles of sodium alginate that have not melted may have been a contributively to the stretching, and fermentation behaviours, as they may be more potent in chemical strength.
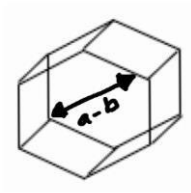
Figure 4-23: Illustration of the a-b plane.

| a) | b) | c) |
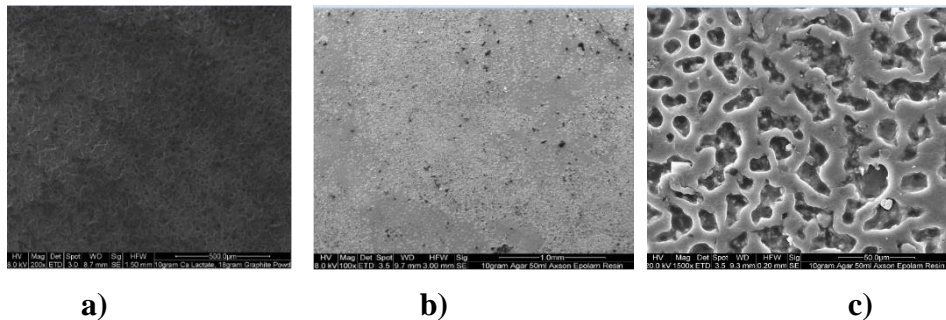
Figure 4-24: (a) The morphology of Experiment 2E SEM (500.µm) of calcium lactate, (b) the morphology of Experiment 3E SEM (1.0mm) of agar, the morphology of Experiment 3E SEM (50.0µm) of agar.

In figure 4-24: (a) this specimen displays air pocket bubbles uniformly throughout the image. This suggests some form of chemical reaction took place during manufacture, and during cure, thus producing gaseous reactivity. The gum-like stretching of the blend mix, influenced by mechanical exfoliation at low (RPM), and intercalation processing shows that the blend mix experienced unique mixing with the use of natural, and synthetic ingredients. The tolerance levels of both the synthetic matrix, and the natural versus synthetic filler challenged the overall cohesion of the blend mix. However, crash out of blend mix was avoided, as the experiment was performed at room temperature.

In figure 4-24: (b) this image shows wide distribution of bubbling effect, suggesting chemical reactions as ingredients subside to the base of the mould. This chemical reaction caused air bubbles to escape piercing through the top plane of the composite.

The magnification in this image is at 1mm, when compared to figure 4-24: (a) where the magnification is at 500µm. The comparison of the two images is that in the agar experiment where the air pockets have broken the epoxy seal figure 4-24: (b) are much denser, and visible. Also, in the case of the agar sample, there appears to be less stretching of the blend mix caused when the air pockets escape from the composite. This is also dependant on the ingredients used.

In figure 4-24: (c) the morphology of the air bubbles displays a lack of conductivity on the outer regions. This means that at the resistance measurement interface there are layers of insulative ingredients that break the platelet-to-platelet interactions. Whilst for softening purposes the ingredients used may make the composite malleable to softening due to unstable chemical or epoxy links.

a)   b)
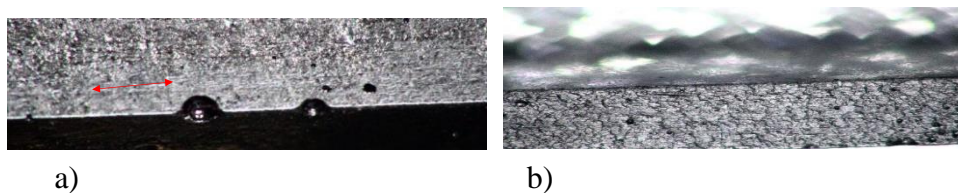
Figure 4-25: (a) Sample 1 Experiment 1A, xGnP (linear layering), (b) Sample 1 Experiment 1A, xGnP (reflectivity behaviour), both taken using Tagarno FHD Trend.

Here in figure 4-25: (a), the linear layering of the nanoplatelets is clearly visible, with nanoplatelets subsiding to the base of the mould, thus taking shapes in the rheology of the formerly wet blend mix. This means that the weight of the platelets dominates the configuration of the majority of the platelets within the composite This sample is now cured, where compression of epoxy between the platelets, and sedimentation has taken place. Planar stratification of xGnP is prevalent.

In figure 4-25: (b) highlight the way that the platelets reflect light maybe useful for the reflection of EMI. As in order to attenuate EMI it is essential to either reflect or absorb the undesired radiated EMW. This shine reflectivity behaviour may be additional, and new information as the reflectivity of the xGnP nanoplatelets has not been studied in this way previously. The refractive index of carbon is n= 2.4168.
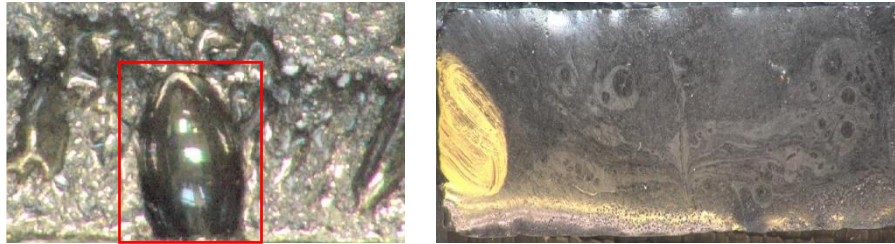
a)   b)

Figure 4-26: (a) Sample 1 Experiment 4C (upturned), (b) Sample 1, Experiment 4D, SG (long reflection), both images are taken using Tagarno FHD Trend.

In figure 4-26: (a) this image shows reflectivity, and there are other images that also show mirror-like reflectivity, yet the image reflected is upside down. This is the big air bubble pocket that demonstrates smooth mirror shine with no hard ridges. This could mean that xGnP could be used in transparent electronic devices that maximise the use of the colour reflectance the graphite emits. The behaviour of the reflection of the platelets shows smooth shine in the big air pocket. This image also shows metallic colouring density throughout the side plane of the specimen, which is evident in groupings of platelet clusters.

Here in figure 4-26: (b) this image shows a long reflection of the metallic pen with which I had dotted the topside of the sample. This could present an interesting factor of the ability to reflect interference out of the composites, as one of the ways to shield against interference is through reflection of the undesired electromagnetic wave. Furthermore, graphite and graphene are anisotropic materials. This anisotropic

phenomenon needs to be further investigated, as the idea of graphite or graphene having different measurements in different directions due to their inherent property, maybe a means to reflect EMI in different directions.

a)   b)
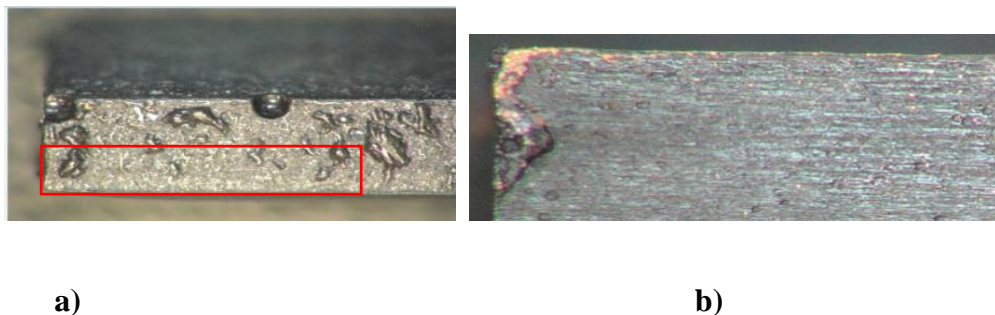
Figure 4-27: (a) Sample Experiment 4C, xGnP (iridescent), (b) Sample 1 Experiment 3B, SG (reflectance gamut) using Tagarno FHD Trend.

In figure 4-27: (a) this sample shows iridescence due to the reflection of light on the sample, and to help this further is the metallic like properties of graphene. The xGnP display colours of green, pink, and yellow colour reflectance. Towards the bottom of the sample, thick layers are visible. This is due to the lack of high (RPM) mechanical exfoliation, where the heavier platelets sediment to the base of the mould. However, further research needs to be undertaken to achieve a more objective inspection.

In figure 4-27: (b) the top left corner of this sample shows a colourful gamut of reflectance, in the yellow/orange/ red hues. The observed morphology of SG through the Tagarno microscopy show thick flat flakes in linear layering.

a)   **b)**
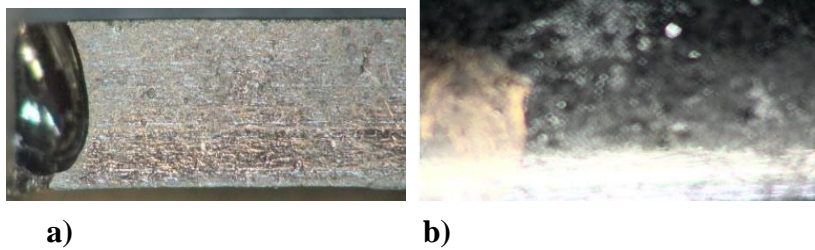
Figure 4-28: (a) Experiment 4A, xGnP (upturned), (b) Experiment 2B, SG (sparkle) using Tagarno FHD Trend.

In figure 4-28: (a) the reflectance of laboratory worker is upturned at an angle. In addition, this image clearly shows the flat sheets of the xGnP platelets that progressively become more condensed to the base of the mould, and sample. Indicating ineffective dispersion through mechanical exfoliation. However, mixing through means of intercalation as described by Pierson (1993) is successfully achieved. This is by means of insertion of a foreign species into the matrix where the four stages of the intercalation compound are progressively carried out. Throughout, the entirety of the experiments within this research successful intercalation combing has been achieved. This extent depends on the ingredients used, and the temperature that the blend mix has been subjected to.

In figure 4-28 (b) displays further imaging of high sparkle, and reflectance of light, combined with shades of green, light blues, and silver. A halo-effect on the SG platelets is shown here, where the outer sides of the platelets show a pink halo followed by luminant bright yellow, green tones. The study of this halo effect maybe useful for the conduction property of the platelets, which need to be aligned to create the situation for electricity to travel through.

a)   b)   c)
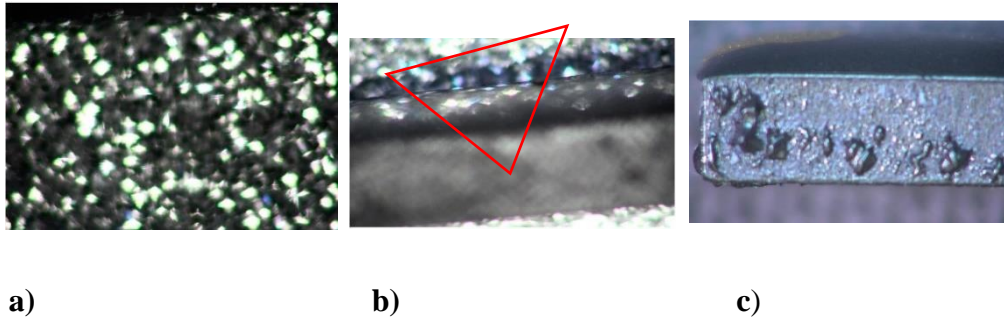
Figure 4-29: (a) Experiment 2B, SG (high sparkle), (b) Experiment 2B, SG (glitter card reflectance), (c) Experiment 2C, xGnP (natural light), all using Tagarno FHD Trend).

In figure 4-29: (a) a higher zoom of graphene platelets, full of sparkle, shine, and colour. This was achieved using a glitter card, and this is the reflectance behaviour. Here the colour that the platelets are showing up on reflectance of light is a potent green. This may be to do with the behaviour of the platelets under certain light conditions. This reflectance behaviour needs to be further studied using objective instrumentation.

In figure 4-29: (b) demonstrates the high level of reflectance within the platelets, able to create mirror-like shine, and sparkle with iridescence, using the technique of a glitter card. It is important to note that the shape of the glitter platelets is circular, whilst the angle of the platelets that reflect the light are at 90°. To reiterate the idea of graphene and graphite having an anisotropic physical property, which is the physical property of them having a different value when measured in different directions. This may mean that when an EMI spur is emitted it may be reflected infinitely. The issue with reflection of EMI is that spur has nit decayed through means of dissipation, or absorption. In fact, the reflected spur is still present. So, to reflect a spur in different directions, with different values maybe the beginning to reflect EMI infinitely.

In figure 4-29: (c) here you see the natural reflectance of graphene platelets under natural light, and camera light (not flash). The platelets still bear iridescence, and platelet reflectivity, and colour. Again, the magnetic sharpie pen is reflecting light in a different way to the rest of the frontal plane of the specimen. The halo behaviour of the platelets can be seen here using xGnP filler. They show a very high outer luminance.

All the specimen images using the Targano FHD Trend give the opportunity to study graphene in a different way, that is convenient, and fast. They also show light on the possibility of studying angular, and atomic attraction of the platelets to achieve EMIS. The manufactured composites need to reflect, dissipate, or absorb the undesired EMW. So, the case remains whether the nano-platelets are able to reflect the interference caused by the undesired EMW.

This section on Tagarno FHD Trend attempts at investigating how various parameters affects reflection. It is acknowledged that the surface needs to be of the same specimen plating when using SEM, and the experimental environment is required to be strictly controlled, and preferably to conform to any available standard. This will be adhered to in future research.

Chapter 5 - Conclusions

A variation of composite manufacture techniques were studied, to see if varying temperature and cycles would impact the performance of the composites during testing or composite characterisation methods. The composites manufactured in this research were made from xGnP, synthetic graphite, epoxy resin, agar, calcium lactate and agar. The three main techniques used are standard exfoliation, magnetic stirrer and sonication.

In the case of this project the agitation and exfoliation of the xGnP is intended to free the layers of xGnP into making stronger interfacial adhesion and apply a good level of xGnP dispersion within the solvent that is the epoxy resin. Each platelet is termed an island and the way it links or communicates to another island being another platelet is called island-island interfacial interactions i.e. platelet to platelet.

Through the media of standard electrical mixer, magnetic stirrer, and sonication, it was possible to visually see how the sedimentation of the filler would de-homogenise partially by mounting the heavier platelets up on top of each other, dictated by heaviest first. Where processing consisted of 3 rounds the sedimentation was disrupted by the exfoliation of the mechanical stirrer. The job of the magnetic stirrer and the sonicator is to intercalate the platelets, while the mechanical stirrer is to exfoliate. The means by which they intercalate is the magnetic stirrer is investigated whether the magnetic properties of graphene, and graphite are influenced by the magnetism of the magnetic stirrer, thus, enabling the platelets to subside layer by layer; graphite or graphene being the first layer in the a-b plane then epoxy then graphite or graphene platelets then epoxy, this would be repeated throughout the composites thus creating graphite intercalated compound by the insertion of a foreign

species into the matrix. A low mechanical stirrer RPM was used to not disturb the work of intercalation. Graphene and SG are reported to have directional magnetic properties (Pierson, 1993).

The purpose of the magnetic stirrer is to excite this behaviour through magnetism, and to see it if it is a property that can lead to better composite conductance. Whilst the sonicator was used to effect and manipulate the empty valence band that cause the high electrical resistance, which there are no reported literature.

It may be that in order for the interfacial adhesion of the resin/hardener to be sufficient so as not to create dams within the nanocomposite the pH value of the resin/hardener would need to be tested and the intermolecular forces would need to be surveyed. This would be done using a field emission scanning electron microscope. The hybridised version of the nanocomposites would be to assess the effects using two different sized xGnP on the rate of electrical field, specific to conductivity as this initiates as to where the conductivity is taking place at the valence band, or as semiconductor would at the band gap. Through this analysis I would be able to test how having a set of conditions for hybridised graphene nanoplatelets would affect the shielding effectiveness of xGnP and the measured electromotive force, measured in volts symbol V.

A high aspect ratio is where the length of the nanoparticle is many times its width, so, a hexagon is equal in width and height. A high surface area is where the thickness is considerably smaller than the surface area. The M25 xGnP grade has a high surface with small thickness whilst the aspect ratio of a hexagon is equal; 25µm. Furthermore, this research was undertaken to examine whether a thermoset resin could be manipulated into softening, evidenced using tensile data analysis, where in some conditions i.e., 1E, 2E ductility was exhibited. This could mean that thermoset

resins could be able to be reheated and recycled, though thermal analysis was not undertaken. The aim was partially achieved with the alignment of the platelets whilst avoiding platelet destructive manufacturing processes, as graphite can be influenced by its geometric morphology in relation to other graphite platelets in creating a conductive network path for electricity to flow through and not be barred by the insulative epoxy.

However, the overall aim of attenuating or eliminating EMI was not achieved. Future work would examine the alignment of the platelets so that there are no vacancy holes within the conductive network path.

5.1 Microscale

Sedimentation: weight of nanoparticles take effect and cause a drooping effect of xGnP to suspend onto the base of beaker where agglomerations of xGnP aggregates descend to the base, this was evident specifically during and post degassing. Thus, this was not a desirable chemical suspension of nanoparticles. This is evidenced in chapter 4.1 Visual Inspection of Mixtures.

Temperature; as the temperature of the blend mix falls to 24°C or below the chemical suspension of the xGnP within resin/hardener becomes heterogenic, and so blocks the prospect of forming cross link chains of polymers, therefore negatively affecting the interfacial adhesion of the blend mix. This then impacts the electron tunnelling theory that pertains to the percolation theory of a conductive network path for electricity to be propagating through the final specimen/medium (He et al., 2017).

5.2 Conductivity

The composites in this research did not achieve consistent conductivity, due to a lack of strong interface bonding as weak interface were exhibited. This can be exhibited in chapter 4.3 Conductivity Results**.** This means a lack of successful load transfer of electric current. Furthermore, because of sedimentation, and the lack of surfactants, air bubbles were an issue that removed access for electricity to find its easiest or fastest route. However, utilising subtle polishing techniques, the electrical conductivity of the xGnP samples were found to be highly conductive, bearing near to zero resistance. The data does not show this as the measurement of resistance was carried out in one specific way for this research, but when light polishing was investigated, this revealed high conductance to some specimens. Another barrier to conductance of the specimens was the insulative nature of epoxy, that blocks interface bonding. Another alternative to epoxy is polystyrene. The thermal conductivity of polystyrene can be reduced with just 2 wt% of graphite (Gong et al., 2015).

The amount of mechanical stirring required to mix the hardener, once the fully processed blend was cooled, lowered the nano mixes' electrical connectivity visibly (a to c axis) which is dependent on the thermal conductivity. As the platelets became less aerated and the blend mix sedimented into the composite moulds this resulted in the blend mix to settle during cure, predominantly in the a to b axis. Due to loss of thermal conductivity which reflects the cohesion and adhesion of the blend mix, as the stronger the interfacial adherence of the xGnP to the xGnP platelets or the SG to the other SG platelets, the greater chance of electrical conductance. However, the insulative nature of the epoxy makes electrical conductivity impossible, as the interface of the platelets with epoxy is greater than with other platelets.

In literature, it has been proven that when the graphene nanoplatelets of the blend ratio are at 10%, this reduces the agglomeration rates to some degree (Kuester et al., 2017). It is a challenge to individualise SG and xGnP filler. Therefore, it may be said that to ensure that platelets are disaggregated would involve the research into a variety of nano composite manufacture with a particular attention to magnetic influence.

The aim was to achieve conductivity on some level within all my experiments. Other aims included to influence the behaviour of the composites with compostable added ingredients through softening of the thermoset plastic, and to achieve some level of ductility on the same samples. These two latter aims were achieved (of softening and ductility) but require further investigation, experimentation, and testing. However, conductivity was not achieved, as the samples were highly insulative due to lack of proper dispersion of the platelets, which lead to clustering and agglomeration. This was a direct result of the use of a standard electrical mixer rather than a high shear mixer. Thus, in future I would compare similar manufacturing processes but with some form of a high shear mixer. The colours reflected by the graphite platelets (be it natural or synthetic) have similar colours to other forms of energy i.e., gas, and electricity. This may mean that they have similar properties. Conversely, the alignment of the platelets was achieved to some extent as the platelets were aligned thoroughly within the conductivity tested specimens Figure 4-28: (a).

5.3 Processing and Manufacturing

The main practicality of using these lengthy, shape-retaining processes during the manufacturing of composites was to maintain the shape of the platelets, and not allow the morphology to get exhausted. However, on the contrary, agglomerations were prevalent due to decision not to use high shear mixing, where high revolutions per

minute that create the case of exfoliation to separate the nano platelets that can also cause deformation, and undesired abrasion of the nanoplatelets. As a result, deformation of the platelets did not occur, but they were not well dispersed. However, the mix was stable, except up on sustained subjection to highest temperatures such as Composite Manufacture Three (Experiments 4C, and 4D) that had encountered near crash out. Furthermore, Composite Manufacture One (Experiment 8E) had experienced crash out, due to incompatible dispersion where no SG was used, where SG had given prior experiments processes stability those that were manufactured, previously.

The platelets had successfully retained their shapes, and morphology. The benefit of this process control was the layering rheology of the platelets had become visible without a microscope as they had sediment to the base of the silicon mould. Thus, the method of utilising intercalation to create the four stages intercalated compound (Pierson, 1993), involving the layering of the foreign species within the matrix did work. The intercalation of graphene or graphite compounds does produce a layered composite in the a-b plane. However, more work needs to be done to create a conducting path.

5.4 Limitations of work

The lack of access to machinery that caused a restriction to the research included the lack of access to a high shear mixer, which persuaded to research other means of composite mixing and manufacture.

Other restrictions to the access of instrumentation that caused a limitation to the research is a lack of a working degassing oven. This machinery removes gases from the blend mix, thus making a more likely outcome of better conductance.

Penultimately to last, the lack of access to a transmission electron microscopy limited the analysis of the blend mix during manufacture, and before the hardener added for cure. Lastly, the lack of time, and organisation of time with microscopy equipment that would provide a controlled environment for specimen, and blend mix inspection.

5.5 Suggestions for future work

- To inspect and assess the success of using other forms of shear mixing i.e., an emulsifying high shear mixer, to provide a comparison to a square hole high shear mixer.

- To ascertain access to a working degassing oven or other degassing instrumentation ahead of composite manufacture.

- To assign a specific amount of time on the study of microscopy required to assess the blend mix and specimens.

Reference List

1. Acharya, S. and Datar, S., 2020. Wideband (8–18 GHz) microwave absorption dominated   electromagnetic interference (EMI) shielding composite using copper aluminum ferrite and reduced graphene oxide in polymer matrix. *Journal of Applied Physics*, *128*(10), p.104902.

2. Alexandre, M., Dubois ,P.,2000. Polymer-layered silicate nanocomposites: preparation, properties and uses of a new class of materials. *Mater Sci Eng*, *28*:1–63.

3. Anwar ,Z., Kausar ,A., Muhammad ,B., 2016. Recent Developments in Epoxy/Graphite, Epoxy/Graphene, and Epoxy/Graphene Nanoplatelet Composites: *A Comparative Review:*
    Polymer-Plastics Technology and Engineering, 55(11). 1192-1210.

4. Anwar ,Z., Kausar ,A., Rafique ,I., Muhammad ,B.,2016. Advances in Epoxy/Graphene Nanoplatelet Composite with Enhanced Physical Properties: A Review. *Polymer-Plastics Technology and Engineering. 55*(6): 643-662.

5. ASTM D638- 14. Standard Test Method for Tensile Properties of Plastics. ASTM. U.S. 2014

6. ASTM E1851-15 Standard Test Method for Electromagnetic Shielding Effectiveness of Durable Rigid Wall Relocatable Structures

7. Atkins, A.G., Atkins, T. and Escudier, M., 2013. *A dictionary of mechanical engineering*. Oxford University Press.

8. Bass, M., Van Stryland, E.W., Wolfe, W.L. and Williams, D.R. eds., 1995. *Handbook of Optics: Fundamentals, techniques, and design*. McGraw-Hill Professional Publishing.

9. Belay, M., Nagarale, R.K. and Verma, V., 2017. Preparation and characterization of graphene-agar and graphene oxide-agar composites. *Journal of Applied Polymer Science*, *134*(33), p.45085.

10. Bradley, A . 2012. *Disaster preparedness for EMP Attacks and solar storms*. USA

11. Campbell Jr, F.C. ed., 2003. *Manufacturing processes for advanced composites*. elsevier.

12. Carr, J., 2000. *The Technician's EMI handbook: Clues and solutions*. Elsevier.

13. Composite EMI Shield. (2004). US2004/0172502 A1.

14. Cubberly, W.H. ed., 1988. *Comprehensive Dictionary of Instrumentation and Control: Reference Guides for Instrumentation and Control*. Instrument Society of America.

15. Davis, J.R. ed., 2004. *Tensile testing*. ASM international.

16. Drakakis, E., Suchea, M., Tudose, V., Kenanakis, G., Stratakis, D., Dangakis, K., Miaoudakis, A., Vernardou, D. and Koudoumas, E., 2018. Zinc oxide-graphene based composite layers for electromagnetic interference shielding in the GHz frequency range. *Thin Solid Films*, *651*, pp.152-157.

17. Drzal, L. (2006). '*Exfoliated Graphite Nanoplatelet (xGnP) A Carbon Nanotube Alternative for Modifying the Properties of Polymers and Composites*. Michigan State University Published.

18. Kim, S., Seo, J. and Drzal, L.T., 2010. Improvement of electric conductivity of LLDPE based nanocomposite by paraffin coating on exfoliated graphite nanoplatelets. *Composites Part A: Applied Science and Manufacturing*, *41*(5), pp.581-587.

19. Garnish, E.W., 1972. Chemistry and properties of epoxide resins. *Composites*, *3*(3), pp.104-111.

20. Geetha, S., Satheesh Kumar, K.K., Rao, C.R., Vijayan, M. and Trivedi, D.C., 2009. EMI shielding: Methods and materials—A review. *Journal of applied polymer science*, *112*(4), pp.2073-2086.

21. Gong, P., Buahom, P., Tran, M.P., Saniei, M., Park, C.B. and Pötschke, P., 2015. Heat transfer in microcellular polystyrene/multi-walled carbon nanotube nanocomposite foams. *Carbon*, *93*, pp.819-829.

22. Gui, D., Gao, X., Hao, J. and Liu, J., 2014. Preparation and characterization of liquid crystalline polyurethane-imide modified epoxy resin composites. *Polymer Engineering & Science*, *54*(7), pp.1704-1711.

23. Gurusideswar, S., Srinivasan, N., Velmurugan, R. and Gupta, N.K., 2017. Tensile response of epoxy and glass/epoxy composites at low and medium strain rate regimes. *Procedia engineering*, *173*, pp.686-693.

24. He, S., Zhang, J., Xiao, X., Hong, X. and Lai, Y., 2017. Investigation of the conductive network formation of polypropylene/graphene nanoplatelets composites for different platelet sizes. *Journal of Materials Science*, *52*(22), pp.13103-13119.

25. Hörold, S., 1999. Phosphorus flame retardants in thermoset resins. *Polymer Degradation and Stability*, *64*(3), pp.427-431.

26. (Jiaming et al., 2016).

27. Jun, Y.S., Um, J.G., Jiang, G. and Yu, A., 2018. A study on the effects of graphene nanoplatelets (GnPs) sheet sizes from a few to hundred microns on the thermal, mechanical, and electrical properties of polypropylene (PP)/GnPs composites. *Express Polymer Letters*, *12*(10), pp.885-897.

28. Justia Patents. 'Patents by Inventor Martin Rapp'; Composite EMI shield. (2003) 20040020674. Available at: https://patents.justia.com/inventor/martin-rapp (Accessed :19th February 2018).

29. Kuester, S., Demarquette, N.R., Ferreira Jr, J.C., Soares, B.G. and Barra, G.M., 2017. Hybrid nanocomposites of thermoplastic elastomer and carbon nanoadditives for electromagnetic shielding. *European Polymer Journal*, *88*, pp.328-339.

30. Kumar, V., Kalia, S. and Swart, H.C. eds., 2017. *Conducting Polymer Hybrids*. Switzerland: Springer International Publishing.

31. Lee, H. and Neville, K., 1967. Handbook of epoxy resins.

32. Madera-Santana, T.J., Misra, M., Drzal, L.T., Robledo, D. and Freile-Pelegrin, Y.J.P.E., 2009. Preparation and characterization of biodegradable agar/poly (butylene adipate-coterephatalate) composites. *Polymer Engineering & Science*, *49*(6), pp.1117-1126.

33. Max Planck Institute, 2018. 'Electron Tunnelling'. Available from: http://www2.fkf.mpg.de/ga/research/stmtutor/stmtheo.html

34. Milton, G.W. and Sawicki, A.T., 2003. Theory of composites. Cambridge monographs on applied and computational mathematics. *Appl. Mech. Rev.*, *56*(2), pp.B27-B28.

35. Morena, J.J., 1997. *Advanced composites world reference dictionary*. Krieger Publishing Company.

36. Nanocomposite Method of Manufacture. (2014). US 8,648,132 B2.

37. Parameswaranpillai, J., Hameed, N., Pionteck, J. and Woo, E.M. eds., 2017. *Handbook of Epoxy Blends*. New York: Springer.

38. Pubchem (2020). Available at: https://pubchem.ncbi.nlm.nih.gov/compound/2286#section=Top (Accessed: 4th August 2020).

39. Pelton, J.N., Madry, S. and Camacho-Lara, S. eds., 2013. *Handbook of satellite applications*. New York: Springer.

40. Pubchem (2020). Calcium Lactate, Sodium Alginate, Agar, epoxy ingredient molecular information. Available from: https://pubchem.ncbi.nlm.nih.gov/ (Accessed: 28th July 2020).

41. Pierson H. 1993. Handbook of Carbon, Graphite, Diamond and Fullerenes: Properties, processing and Applications. Park Ridge, New Jersey, United States of America: Noyes Publications.

42. Ragan, S. and Marsh, H., 1983. Science and technology of graphite manufacture. *Journal of materials science*, *18*(11), pp.3161-3176.

43. Rennie, R. and Law, J. eds., 2016. *A Dictionary of Chemistry*. Oxford University Press.

44. Ren, Y., Guo, H., Liu, Y., Lv, R., Zhang, Y., Maqbool, M. and Bai, S., 2019. A trade-off study toward highly thermally conductive and mechanically robust thermoplastic composites by injection moulding. *Composites Science and Technology*, *183*, p.107787.

45. Schoen, S., 2016. *Newton's telecom dictionary*. Telecom Publishing.

46. Sedlarik, V., Galya, T., Emri, I. and Saha, P., 2009. Structure and conditioning effect on mechanical behavior of poly (vinyl alcohol)/calcium lactate biocomposites. *Polymer Composites*, *30*(8), pp.1158-1165.

47. Sevkat, E. and Brahimi, M., 2011. The bearing strength of pin loaded woven composites manufactured by vacuum assisted resin transfer moulding and hand lay-up techniques. *Procedia Engineering*, *10*, pp.153-158.

48. Sharma, S.K., Gupta, V., Tandon, R.P. and Sachdev, V.K., 2016. Synergic effect of graphene and MWCNT fillers on electromagnetic shielding properties of graphene–MWCNT/ABS nanocomposites. *RSC advances*, *6*(22), pp.18257-18265.

49. Song, W.L., Cao, M.S., Lu, M.M., Yang, J., Ju, H.F., Hou, Z.L., Liu, J., Yuan, J. and Fan, L.Z., 2013. Alignment of graphene sheets in wax composites for electromagnetic interference shielding improvement. *Nanotechnology*, *24*(11), p.115708.

50. Thomassin, J.M., Jerome, C., Pardoen, T., Bailly, C., Huynen, I. and Detrembleur, C., 2013. Polymer/carbon based composites as electromagnetic interference (EMI) shielding materials. *Materials Science and Engineering: R: Reports*, *74*(7), pp.211-232

51. Tokala, M.R., Padya, B., Jain, P.K. and Chakra, C.S., 2015. Preparation and characterization of graphene nano-platelets integrated polyaniline based conducting nanocomposites. *Superlattices and Microstructures*, *82*, pp.287-292.

52. Tomsic, J., 2000. *Dictionary of materials and testing* (pp. i-vii). SAE.

53. Tong, X.C., 2016. *Advanced materials and design for electromagnetic interference shielding*. CRC press.

54. Wang, W., Cui, R., Zhang, P., Wan, C. and Pan, W., 2021. High electromagnetic interference shielding effectiveness in MgO composites reinforced by aligned graphene platelets. *Journal of the American Ceramic Society*, *104*(6), pp.2868-2878..

55. Weik M. 1996. Communications Standard Dictionary. New York, Albany, Bonn, Boston, Cincinnati, Detroit, London, Madrid, Melbourne, Mexico City, Pacific Grove, Paris, San Francisco, Singapore, Tokyo, Toronto, Washington: International Thomson Publishing.

56. Wu, J., Chen, J., Zhao, Y., Liu, W. and Zhang, W., 2016. Effect of electrophoretic condition on the electromagnetic interference shielding performance of reduced graphene oxide-carbon fiber/epoxy resin composites. *Composites Part B: Engineering, 105*, pp. 167-175.

57. Yadav, R.S., Kuritka, I. and Vilcáková, J., 2020. *Advanced Spinel Ferrite Nanocomposites for Electromagnetic Interference Shielding Applications*. Elsevier.

58. Zaman, I., Phan, T.T., Kuan, H.C., Meng, Q., La, L.T.B., Luong, L., Youssf, O. and Ma, J., 2011. Epoxy/graphene platelets nanocomposites with two levels of interface strength. *Polymer*, *52*(7), pp.1603-1611.

59. Zhou, F., Feng, X., Yu, J. and Jiang, X., 2018. High performance of 3D porous graphene/lignin/sodium alginate composite for adsorption of Cd (II) and Pb (II). *Environmental Science and Pollution Research*, *25*(16), pp.15651-15661.